

# Lawrence Berkeley National Laboratory

## Recent Work

### Title

COMPOSITENESS, FEYNMAN DIAGRAMS, AND THE REGGEIZED ABSORPTION MODEL

### Permalink

<https://escholarship.org/uc/item/8jd785s1>

### Author

Risk, Clifford.

### Publication Date

1970-06-08

Submitted to Physical Review

UCRL-19831  
Preprint

c. 2

**RECEIVED  
LAWRENCE  
RADIATION LABORATORY**

JUL 30 1970

**LIBRARY AND  
DOCUMENTS SECTION**

COMPOSITENESS, FEYNMAN DIAGRAMS,  
AND THE REGGEIZED ABSORPTION MODEL

Clifford Risk

June 8, 1970

AEC Contract No. W-7405-eng-48

**TWO-WEEK LOAN COPY**

*This is a Library Circulating Copy  
which may be borrowed for two weeks.  
For a personal retention copy, call  
Tech. Info. Division, Ext. 5545*

31 a **LAWRENCE RADIATION LABORATORY**  
**UNIVERSITY of CALIFORNIA BERKELEY**

UCRL-19831

*cy*

## **DISCLAIMER**

This document was prepared as an account of work sponsored by the United States Government. While this document is believed to contain correct information, neither the United States Government nor any agency thereof, nor the Regents of the University of California, nor any of their employees, makes any warranty, express or implied, or assumes any legal responsibility for the accuracy, completeness, or usefulness of any information, apparatus, product, or process disclosed, or represents that its use would not infringe privately owned rights. Reference herein to any specific commercial product, process, or service by its trade name, trademark, manufacturer, or otherwise, does not necessarily constitute or imply its endorsement, recommendation, or favoring by the United States Government or any agency thereof, or the Regents of the University of California. The views and opinions of authors expressed herein do not necessarily state or reflect those of the United States Government or any agency thereof or the Regents of the University of California.

COMPOSITENESS, FEYNMAN DIAGRAMS,  
AND THE REGGEIZED ABSORPTION MODEL

Clifford Risk

Lawrence Radiation Laboratory  
University of California  
Berkeley, California

June 8, 1970

ABSTRACT

In this paper we derive the Reggeized absorption model from field theoretic diagrams. This model has been used to describe a large number of quasi-two-body reactions. It involves a Regge cut correction to Regge pole amplitudes which is generated by the exchange of the Regge pole and a Pomeron. The cut features the product of the Reggeon and Pomeron (without complex conjugation of either) and a large magnitude for the cut (coherent inelastic effects add to the original cut term).

The fundamental physical assumption of our derivation is that physical particles are composite objects of constituent pieces of matter. In a scattering process, some of the constituent matter takes part in the scattering while the rest stands by as a spectator. These ideas lead us to describe double scattering processes by a class of

diagrams involving exchange of two Reggeons in the cross channel and propagation of composite physical particles in the direct channel. When the direct-channel particles are Reggeized, we obtain an expression for the Regge box diagram.

We begin our analysis of diagrams by discussing the AFS diagram and similar diagrams to demonstrate how the absence of third double-spectral functions leads to the absence of a cut. For simple diagrams, we find that we are forced to invoke properties of form factors to show absence of the cut, but that for sufficiently composite diagrams the absence of the cut rests solely on the absence of the third double-spectral functions.

Next we discuss the Mandelstam diagram and similar diagrams to demonstrate how the presence of third double-spectral functions leads to cuts. For each diagram we bring the expression for the amplitude to the form of the absorption model.

Finally, we study the general class of diagrams referred to above. These diagrams feature compositeness in the direct channel (physical particles are composite), third double-spectral functions (physical particles have definite signature; no exchange degeneracy), and two-Reggeon exchange (double scattering and the Glauber spectator approximation). By assuming saturation of direct-channel amplitudes by physical states, we are led to an absorption formula (no complex conjugations) that includes the coherent inelastic factor  $\lambda$  (diffraction production of direct-channel resonances).

## I. INTRODUCTION\*

The idea that the asymptotic behavior of a scattering amplitude  $A(s,t)$  is determined by singularities of the partial-wave amplitude  $f_j(t)$  in the complex  $j$  plane is ten years old.<sup>1</sup> During this decade, this idea has been studied both phenomenologically with various models that describe specific reactions,<sup>2</sup> and theoretically with the investigation of sums of Feynman diagrams that define amplitudes with various types of  $j$ -plane singularities.<sup>3,4</sup>

The main school of thought has been that  $f_j(t)$  is meromorphic in the  $j$  plane with simple poles at values  $j = \alpha_i(t)$  that correspond to physical particles. Phenomenological models with these Regge poles were used to fit a large number of elastic and quasi-two-body reactions. Meanwhile, the theoretical study of various field theories led to the conclusion that Regge poles arise in field theories also.

However, the use of phenomenological models with poles alone led to several difficulties and complications in the attempt to explain features of differential cross sections<sup>5</sup>-such as dips, crossovers, and forward peaks (in  $\pi$  exchange reactions)-and features of total cross sections-such as the rise at Serpukhov energies. This suggested that in the  $j$  plane the properties of  $f_j(t)$  might be more involved than containing poles only. Meanwhile, the study of field-theory models produced amplitudes with fixed poles, moving cuts, fixed cuts, and essential singularities.<sup>3</sup>

One of the earlier models with more complicated singularities was developed by Abers<sup>6</sup> et al. (following earlier work by Udgaonkar

and Gell-Mann<sup>7</sup>) in the study of  $\pi$ -deuteron scattering. Glauber<sup>8</sup> had shown that the amplitude  $A_{\pi d}$  could be expressed as a sum of single and double  $\pi N$  scatterings. Abers et al. then showed that these scatterings correspond to the amplitudes for the diagrams of Fig. 1, where the particles in the direct channel (cut by the dashed line) are to be evaluated near mass shell. Furthermore, if the single scattering terms were given by Regge poles

$$A_{\pi p}(s, t) = \beta(t) s^{\alpha(t)}, \quad (1)$$

then the double scattering term of Eq. (1) took the form of an amplitude with a cut in the  $j$  plane at  $j(t) = 2\alpha\left(\frac{t}{4}\right) - 1$ ,

$$A(\text{double}) = \frac{s^{j(t)}}{\ln s}. \quad (2)$$

This cut term, the Glauber shadow correction, was observed experimentally in differential and total cross sections. However, it was next shown that if in Fig. 1b the contribution was evaluated from the region of integration where the  $\pi$  was off mass shell, this exactly canceled the cut. The sum of both contributions behaved as  $\ln s/s^3$  and had no leading cut.<sup>9</sup>

This type of theoretical difficulty also occurs in models that describe two-body processes in terms of a multiple scattering series. In describing  $\pi^- p \rightarrow \pi^0 n$ , one is led to the formula<sup>5</sup> (where  $A_{el} \sim -i$ )

$$A(s, t) = A_0(s, t) - \frac{i}{32\pi^2} \int d\Omega A_0(s, t_1) A_{el}(s, t_2), \quad (3)$$

where  $A_\rho$  is the amplitude for  $\rho$  exchange, and  $A_{el}$  is the elastic  $\pi$ -nucleon amplitude. This can be derived from either a Glauber eikonal series<sup>10,11</sup> or from the Sopkovitch formula.<sup>5</sup> It can also be derived from Feynman diagrams of the type of Fig. 2b. The second term in Eq. (3) corresponds to the contribution from Fig. 2b in which the direct channel  $\pi^0, n$  are evaluated on mass shell. However, if one evaluates the contribution from the region where the  $\pi^0, n$  go off mass shell, the previous term is again exactly canceled, and their sum has no cut.

The difficulty encountered in both of these examples is related to the diagram version of the work of AFS. The discontinuity of the amplitude of Fig. 3 across the branch cut of the two-particle direct-channel state is given by<sup>12</sup>

$$\text{Im } A(s, t) \propto \int \frac{d^2 \tilde{k}}{s} A_1(s, t_1) A_2^*(s, t_2) \quad , \quad (4)$$

and  $A(s, t)$  has a branch point at  $j(t) = 2\alpha(t/4) - 1$ . However, in a ladder representation of a Reggeon,<sup>13</sup> there are further contributions to the unitarity equation that cancel the cut.<sup>14</sup>

Although the three diagrams considered do not have cuts, there are diagrams which do have cuts, for example, the double cross diagram<sup>3,15</sup> of Fig. 4.

In this work we will reconcile these results for Feynman diagrams on the one hand with the experimentally valid multiple scattering models on the other. To do this, we start from assumptions about the composite structure of physical particles, and combine them with the ideas of multiple scattering. This leads us to a class of Feynman



diagrams, which can be evaluated in the high-energy limit. The final expression we are led to agrees with the multiple-scattering models discussed above.

The organization of the paper is as follows. In Sec. II A we point out the features of the AFS diagram that cause it not to have a cut. In B we discuss why the double cross diagram of Fig. 4 does have a cut, and bring the amplitude to a form similar to the absorption model. Next we extend the results to more complicated diagrams with cuts. In C we discuss two further diagrams without cuts, drawing out the role that third double-spectral functions and form factors play in the analysis. This leads to the analysis in D of a very general class of diagrams, in which the presence of a cut is thrown completely onto the presence of third double-spectral functions.

In Sec. III we present our view of the composite structure of physical particles and combine this with the diagram results to obtain the derivation of the absorption model.

In Sec. IV we compare our results with the work of Gribov et al.

In Sec. V we summarize the assumptions, results, and unsolved problems of the paper.

## II. MATHEMATICAL DERIVATIONS

### A. The AFS Diagram

To begin we briefly point out the features of Rothe's treatment<sup>16,17</sup> of the AFS diagram that are relevant to our later derivation.

In terms of mass variables, the amplitude is given by

$$A(s,t) \propto \frac{1}{s} \int_{\lambda(t,t_1,t_2) \leq 0} \frac{dt_1 dt_2}{(-\lambda)^{\frac{1}{2}}} \int_{\lambda(s,s_1,s_2) \geq 0} ds_1 ds_2 \quad \times \frac{R(s,t_1; s_1, s_2) R(s,t_2; s_1, s_2)}{(s_1 - m^2 + i\epsilon)(s_2 - m^2 + i\epsilon)}, \quad (5)$$

where

$$\lambda(a,b,c) = a^2 + b^2 + c^2 - 2ab - 2ac - 2bc.$$

As a function of  $s_1$ , the integrand of Eq. (5) has singularities in the lower half plane consisting of a pole at  $s_1 = m^2 - i\epsilon$  and cuts from the form factors of the Regge amplitudes. Also, it is known<sup>14,18</sup> that as  $s_1$  becomes large

$$R(s,t; s_1, s_2) \rightarrow 1/s. \quad (6)$$

(This is valid in the limit  $s$  fixed,  $s_1 \rightarrow \infty$  and also in the limit  $s \sim s_1 \rightarrow \infty$ .) The  $s_1$  integration runs from  $s_1 = -\infty$  to  $s_1 \sim s$  (Fig. 5). Therefore, if we distort the  $s_1$ -and similarly  $s_2$ -integration in the lower half plane, we obtain

$$A(s,t) \propto \frac{1}{s} \int \frac{dt_1 dt_2}{(-\lambda)^{\frac{1}{2}}} R(s,t_1) R(s,t_2) + A_2(s,t) + A_3(s,t), \quad (7)$$

where  $R(s, t_1)$  is the Regge amplitude evaluated on mass shell,  $A_2$  is the contribution from the cuts in the mass variables, and  $A_3(s, t)$  is the contribution from the large semicircles. This last term is negligible because of Eq. (6). The first term in Eq. (7) is the usual AFS amplitude [but without complex conjugation of  $R(s, t_2)$ ].

On the other hand, if we close the contour of  $s_1$  integration in the upper half plane, we obtain for  $A(s, t)$  only a term similar to  $A_3(s, t)$ , which vanishes as  $s \rightarrow \infty$ . Hence we conclude that  $A(s, t)$  must vanish as  $s \rightarrow \infty$ . (the Feynman parameter technique gives  $\ln s/s^3$ ), and the apparent cut of the first term in Eq. (7) is canceled by  $A_2(s, t)$ .

To summarize, the cut does not appear because of

- (a) the absence of a third double spectral function
- (b) the presence of form factors.

We shall see that the correct interpretation of these two features leads to the Reggeized absorption model.

## B. Diagrams With Cuts

We now turn to diagrams that do have cuts, leading to the general diagram of Sec. D that will connect with our ideas of the composite structure of physical particles and yield the absorption model.

First consider the double cross diagram of Fig. 4. We follow the treatment by Gribov (1968),<sup>19</sup> and then extend the analysis further to obtain a result resembling the absorption model. The amplitude of Fig. 4 is given by<sup>16,19</sup>

$$A(s,t) = i \int \frac{d^4 k \, d^4 k_1 \, d^4 k_2}{\prod_1^8 d_i} R(k_1, k_2, k) R'(p_i - k_1, p_2 - k_2, q - k). \quad (8a)$$

The essential feature of the analysis is to note from Eq. (6) that the internal Regge amplitudes  $R$  and  $R'$  become small if their external masses  $d_i$  become large as fast as or faster than  $s$ . Therefore, the dominant contribution to Eq. (8a) comes from the region of integration where  $d_i$  remains finite relative to  $s$  as  $s$  goes to infinity. After  $s$  has become asymptotic, the integration over the remaining large values of  $d_i$  can be completed. To express this precisely, let  $\Lambda$  be a finite number, and define

$$A_\Lambda(s,t) = i \int d^4 k \, d^4 k_1 \, d^4 k_2 R R' \prod_1^8 \frac{\theta(\Lambda - d_i^2)}{d_i}. \quad (8b)$$

Then, the above arguments state the leading behavior of  $A(s,t)$  is given by

$$\lim_{s \rightarrow \infty} A(s,t) = \lim_{\Lambda \rightarrow \infty} \left[ \lim_{s \rightarrow \infty} A_{\Lambda}(s,t) \right]. \quad (8c)$$

To perform the analysis embedded in Eqs. (8a) and (8c), it is convenient to replace the external momenta  $p_1, p_2$  by light-like momenta  $p'_1, p'_2$  defined to order  $1/s$  by

$$p'_1 = p_1 - \frac{m^2}{s} p_2, \quad p'_2 = p_2 - \frac{m^2}{s} p_1.$$

The momentum transfer is given by  $q = \frac{t}{s} (p'_2 - p'_1) + Q$ , where  $Q$  is a two-dimensional vector perpendicular to the incident vectors  $p_1, p_2$ .

The Sudakov variables of integration are introduced by

$$k = \alpha p'_2 + \beta p'_1 + K; \quad k_i = \alpha_i p'_2 + \beta_i p'_1 + K_i, \quad \text{for } i=1,2,$$

$$d^4k = \frac{|s|}{2} d\alpha d\beta dk, \text{ etc.},$$

where  $K, K_i$  are again two-dimensional vectors perpendicular to  $p_1, p_2$ .

In terms of these variables, the denominators for the left side of

Fig. 4 become

$$d_1 = k_1^2 - m^2 + i\epsilon = \alpha_1 \beta_1 s + K_1^2 - m^2 + i\epsilon,$$

$$d_2 = (p_1 - k_1)^2 - m^2 + i\epsilon = \left(\alpha_1 - \frac{m^2}{s}\right)(\beta_1 - 1)s + K_1^2 - m^2 + i\epsilon, \quad (9)$$

$$d_3 = (k_1 - k)^2 - m^2 + i\epsilon = (\alpha_1 - \alpha)(\beta_1 - \beta)s + (K_1 - K)^2 - m^2 + i\epsilon,$$

$$d_4 = (k_1 - k + q - p_1)^2 - m^2 + i\epsilon = \left(\alpha_1 - \alpha + \frac{t}{s} - \frac{m^2}{s}\right)(\beta_1 - \beta - \frac{t}{s} - 1)s + (K_1 - K - Q)^2 - m^2 + i\epsilon,$$

with similar expressions on the right side.

Performing the analysis of Eqs. (8a) and (8b), we first find the region of integration over which  $d_i \leq \Lambda$ . By solving the equations  $d_1, d_2 = O(\Lambda)$  for  $\alpha_1, \beta_1$ , we find from Eq. (14) that  $\alpha_1 = O(\frac{\Lambda}{s})$ ,  $\beta_1 = O(\Lambda)$ . After a similar analysis on  $d_3, d_4$ ;  $d_5, d_6$ ;  $d_7, d_8$ , we conclude that the dominant region of integration as  $s \rightarrow \infty$  is given by

$$\alpha_1, \alpha, \beta, \beta_2 = O(\frac{\Lambda}{s}); \quad \beta_1, \alpha_2 = O(\Lambda). \quad (10)$$

Comparing Eq. (10) with Eq. (9), we see that we can neglect  $\beta$  relative to  $\beta_1$ , and  $\alpha$  relative to  $\alpha_2$ . If we change variables  $\alpha_1 s \rightarrow \alpha_1$ ,  $\alpha s \rightarrow \alpha$ ,  $\beta s \rightarrow \beta$ ,  $\beta_2 s \rightarrow \beta$ , Eqs. (9) become

$$\begin{aligned} d_1 &= \alpha_1 \beta_1 + K_1^2 - m^2 + i\epsilon, \\ d_2 &= (\alpha_1 - m^2)(\beta_1 - 1) + K_1^2 - m^2 + i\epsilon, \\ d_3 &= (\alpha_1 - \alpha)\beta_1 + (K_1 - K)^2 - m^2 + i\epsilon, \\ d_4 &= (\alpha_1 - \alpha + t - m^2)(\beta_1 - 1) + (K_1 - K - Q)^2 - m^2 + i\epsilon, \end{aligned} \quad (11)$$

and the Regge energies, momentum transfers, and direct channel energies become

$$\begin{aligned} U_1 &\rightarrow \alpha_2 \beta_1 s, \quad U_2 \rightarrow (1 - \alpha_2)(1 - \beta_1)s; \\ k^2 &= K^2, \quad (q - k)^2 = (Q - K)^2; \\ s_1 &= m^2 - \alpha + K^2, \quad s_2 = m^2 + \beta + K^2. \end{aligned} \quad (12)$$

The factors  $\alpha_2, \beta_1$ , etc. in Eq. (12) tell what fraction of the original energy  $s$  flows through the Reggeons and what portion flows down the sides of the diagram. We see that the terms  $d_1, \dots, d_4$  depend only on

the variables of the left loop  $\alpha_1, \beta_1, K_1$  and on  $\alpha, K$ , but not on  $\beta$ . Similarly for the terms  $d_5, \dots, d_8$ .

Next we assume that the Regge amplitudes of Eq. (8a) can be written in the factorized form

$$R = g_1(d_1, d_3, k^2) e^{-\frac{i\pi}{2}\phi_1(k^2)} U_1 \phi_1(k^2) g_2(d_5, d_7, k^2)$$

$$R' = g'_1(d_2, d_4, (q-k)^2) e^{-\frac{i\pi}{2}\phi_2[(q-k)^2]} U_2 \phi_2[(q-k)^2] g_2(d_6, d_8, (q-k)^2).$$

Then, Eq. (8a) can be recast into the following form:

$$A_\Lambda(s, t) \propto \int_{0(\Lambda)} dK \left( e^{\frac{i\pi}{2}s} \right)^{\phi_1(K^2) + \phi_2[(Q-K)^2] - 1} N_1(K, Q) N_2(K, Q), \quad (13a)$$

$$N_1(K, Q) = \int_{0(\Lambda)} d\alpha \frac{d\alpha_1 d\beta_1 dK_1}{\prod_1 d_i} g_1 g'_1 \beta_1^{\phi_1} (1 - \beta_1)^{\phi_2}, \quad (13b)$$

$$N_2(K, Q) = \int_{0(\Lambda)} d\beta \frac{d\alpha_2 d\beta_2 dK_2}{\prod_5 d_i} g_2 g'_2 \alpha_2^{\phi_1} (1 - \alpha_2)^{\phi_2}. \quad (13c)$$

Here we see that  $A_\Lambda$  is an integral over the usual energy term  $s^{\phi_1 + \phi_2 - 1}$ , times structure functions  $N_1$  and  $N_2$  that involve the Feynman amplitudes, the form factors, and the Regge energy factors on each side of the diagram.

Now let  $\Lambda \rightarrow \infty$  in accord with Eq. (8c). We denote the integrand of  $N_1$  by

$$A_1(\alpha, K, Q) = \int_{-\infty}^{+\infty} \frac{d\alpha_1 d\beta_1 dK_1}{\prod_1^4 d_i} g_1 g'_1 \beta_1^{\phi_1} (1 - \beta_1)^{\phi_2} . \quad (14)$$

Note from Eq. (14) that  $\beta_1$  runs between 0 and +1 only. If  $\beta_1 < 0$ , then the integrand, as a function of  $\alpha_1$ , has singularities that all lie in the upper half plane [see Eq. (11) and Fig. 6]; the  $\alpha_1$  contour of integration can be closed in the lower half plane to give zero. If  $\beta_1 > 1$ , the singularities all lie in the lower half plane. But if  $0 < \beta_1 < 1$ , then the singularities pinch the contour of integration and the integral is nonzero.

To bring  $A(s, t)$  into the form of the absorption model, we shall find it necessary to understand the analytic properties of  $A_1$ .

This can be investigated in the following way. (We neglect the form factors, which can be handled by dispersing in their masses.<sup>20</sup>) Introduce Feynman parameters<sup>20-22</sup> into Eq. (14) via

$$\prod_{j=1}^4 \frac{1}{d_j} = \left(\frac{1}{i}\right)^4 \int_0^\infty \prod_1^4 d\lambda_j e^{i \sum_1^4 \lambda_j d_j} . \quad (15)$$

(The  $i\epsilon$  in  $d$  guarantees convergence.) Then, the  $dK_1$  integration can be done directly. The  $d\alpha_1$  integration can be done by using

$$\int_{-\infty}^{+\infty} d\alpha e^{i\alpha B} \propto \delta(B) . \quad (16a)$$

The quantity  $B$  involves  $\beta_1$ , and this allows the  $d\beta_1$  integral to be performed. We find



$$\beta_1 = \frac{\lambda_2 + \lambda_4}{\lambda_1 + \lambda_2 + \lambda_3 + \lambda_4}, \quad (16b)$$

and that

$$A_1(s_1, t; t_1, t_2) \propto \int_0^\infty \prod_1^4 d\lambda_j \left( \frac{\lambda_2 + \lambda_4}{c} \right)^{\phi_1} \left( \frac{\lambda_1 + \lambda_3}{c} \right)^{\phi_2} \times \frac{e^{iD(\lambda, s_1, u_1)/C(\lambda)}}{[C(\lambda)]^2}, \quad (17a)$$

where

$$D(\lambda, s_1, u_1) = \lambda_2 \lambda_3 s_1 + \lambda_1 \lambda_4 u_1 + \lambda_1 \lambda_3 t_1 + \lambda_2 \lambda_4 t_2 + m^2(\lambda_1 \lambda_2 + \lambda_3 \lambda_4) - m^2 C(\lambda)^2 \quad (17b)$$

$$C(\lambda) = \lambda_1 + \lambda_2 + \lambda_3 + \lambda_4 \quad (17c)$$

$$s_1 + t + u_1 = 2m^2 + t_1 + t_2. \quad (17d)$$

This can be written in the more familiar Feynman representation as

$$A_1(s_1, t; t_1, t_2) \propto \int_0^1 \prod_1^4 d\alpha_i \delta(1 - c) \left( \frac{\alpha_2 + \alpha_4}{c(\alpha)} \right)^{\phi_1} \left( \frac{\alpha_1 + \alpha_3}{c(\alpha)} \right)^{\phi_2} \times \frac{1}{[D(\alpha, s_1, u_1)]^2}. \quad (17e)$$

Note that for  $\phi_1 = \phi_2 = 0$ ,  $A_1$  reduces to  $\bar{A}_1$ , the ordinary Feynman amplitude of Fig. 7.

From Eq. (17e) the analytic properties of  $A_1$  can be read off instantly. First,  $A_1$  has the same Landau curves as  $\bar{A}_1$ , because these come from  $D(\alpha, s_1, u_1)$ . Second, the term  $\beta_1^{\phi_1}$  does not introduce a new singularity, because if  $\alpha_2 = \alpha_4 = 0$ , then

$$D(\alpha, s_1, u_1) = \alpha_1 \alpha_3 t_1 - (\alpha_1 + \alpha_3)^2 m^2 ;$$

but since  $t_1 < 0$ , then  $D$  is strictly negative and cannot pinch with  $\beta_1^{\phi_1}$ . Finally, it can be seen from Eq. (17b) that for

$$s_1, u_1 \lesseqgtr 2m^2 ,$$

$D$  is strictly negative; therefore  $A_1$  is strictly real there. This region, labelled  $D_2$ , is shown in Fig. 8. We summarize the results in Fig. 9a. The expression for  $A_1$  in Eq. (17e) in terms of invariants also allows us to write

$$A(s, t) \text{ oc } \int \frac{dt_1 dt_2}{(-\lambda)^{\frac{1}{2}}} \left(\frac{s}{i}\right)^{\phi_1(t_1) + \phi_2(t_2) - 1} N_1(t, t_1, t_2) N_2(t, t_1, t_2) \quad (18a)$$

$$N_i(t, t_1, t_2) = \int_{-\infty}^{+\infty} ds_i A_i(s_i, t; t_1, t_2) . \quad (18b)$$

We can now bring  $A(s, t)$  to the form of the absorption model. In Fig. 9a we distort the contour of integration around the right-hand cut.

( $A_1 \rightarrow \ln s_1/s_1^2$  as  $s_1 \rightarrow \infty$ .) Then

$$N_1(t, t_1, t_2) \text{ oc } \int_{4m^2}^{\infty} ds_1 \text{ disc}[A_1(s_1, t; t_1, t_2)] . \quad (19a)$$

Since  $A_1$  is real analytic between the cuts of Fig. 9a, note that

$$\text{disc}[A_1] = 2i \text{ Im } A_1 . \quad (19b)$$

Since the discontinuity is generated by the denominators  $d_2, d_3$ , and since  $A_1$  is real analytic, we can invoke a Cutkosky-type theorem to give

$$N_1(t, t_1, t_2) \propto i \int_{4m^2}^{\infty} ds_1 \int \frac{d\alpha_1 d\beta_1 dK_1}{d_1 d_4} \beta_1^{\phi_1} (1 - \beta_1)^{\phi_2} \delta(d_2) \delta(d_3) F, \quad (19c)$$

where  $F$  involves the Jacobian of the transformation to mass variables.

Integrating on the  $\delta$  functions, we obtain

$$N_1(t, t_1, t_2) \propto i \int_{4m^2}^{\infty} ds_1 \int dK_1 B^U B^{*L} \quad (19d)$$

where

$$B^U = \left. \frac{\beta_1^{\phi_1}}{d_1} (F)^{\frac{1}{2}} \right|_{d_2=d_3=0}, \quad B^L = \left. \frac{(1 - \beta_1)^{\phi_2}}{d_4} (F)^{\frac{1}{2}} \right|_{d_2=d_3=0} \quad (19e)$$

In terms of graphs, we can write  $N_1$  as in Fig. 9b.

Thus we can split  $N_1$  into an integral of factors  $B^U B^{*L}$ , where  $B^U$  involves the upper part of the diagram, and  $B^L$  involves the lower part. Performing the same operation on  $N_2$ .

$$N_2 \propto i \int_{4m^2}^{\infty} ds_2 \int dK_2 C^U C^{*L} \quad (19f)$$

Returning to Eq. (18a), we can bring  $A(s, t)$  to the form

$$A(s,t) \propto \frac{-i}{s} \int \frac{dt_1 dt_2}{(-\lambda)^{\frac{1}{2}}} dK_1 dK_2 \left\{ B^U\left(\frac{s}{i}\right)^{\phi_1(t_1)} C^U \right\} \left\{ B^{L*}\left(\frac{s}{i}\right)^{\phi_2(t_2)} C^{L*} \right\}. \quad (20a)$$

Writing

$$M_1 = B^U\left(\frac{s}{i}\right)^{\phi_1} C^U, \quad M_2 = B^L\left(\frac{s}{i}\right)^{\phi_2} C^L, \quad (20b)$$

we finally arrive (see Fig. 10) at

$$A(s,t) \propto \frac{-i}{s} \int dK dK_1 dK_2 M_1 M_2^* e^{-i\pi\phi_2(t_2)}. \quad (20c)$$

With B,C real, Eq. (20a) agrees with the absorption model. In particular, when  $\phi_1$  is the Pomeranchuk, then  $A(s,t)$  interferes destructively with the pole term of  $\phi_2$ . In Eq. (20c) the extra phase term restores the correct phase to the  $M_2$  amplitude.

To extend this result and prepare for the general diagram of Sec. D, we briefly discuss the diagram of Fig. 11. There are several noteworthy features.

In the first place, one sees that on the left side of the diagram only the lines 1,3,5,7 attach to Regge amplitudes. Hence we might suspect that only these are subject to the finite-mass condition. It turns out this would not give enough conditions to provide an immediate solution for the Sudakov variables. There are two ways we can argue to extend the class 1,3,5,7. On the one hand we can argue that, in the spirit of Arnold, HPKR, and of the work to follow in Sec. III, the external physical particles should themselves also be Reggeized. This would place form factors on the external vertices also, and would

lead to the requirement that the lines 2,6 also satisfy the finite-mass condition, and would provide enough lines to perform the Gribov analysis. On the other hand, Polkinghorne<sup>23</sup> has recently extended the Gribov analysis to diagrams with internal Reggeons constructed from Veneziano amplitudes without any form factors at all. The integrations are done by a steepest-descent analysis, and as it turns out this leads to the desired finite mass conditions on all internal lines.

In any event, after satisfying the finite mass conditions, one finds, in the same way as before,

$$\alpha_1, \alpha_2, \alpha, \beta, \beta_3, \beta_4 \sim \Lambda/s, \quad 0 < \beta_1, \beta_2, \alpha_3, \alpha_4 < 1 .$$

One again obtains the amplitude  $A(s,t)$  in the same form as before, with the amplitude  $A_1(s_1, t; t_1, t_2)$  now given by

$$A(s_1, t; t_1, t_2) = \int_0^1 d\beta_1 d\beta_2 \beta_1^{\phi_1} \beta_2^{\phi_2} g_1 g_2 \int_{-\infty}^{+\infty} \frac{d\alpha_1 d\alpha_2 dK_1 dK_2}{\prod_1 d_i} . \quad (21)$$

The amplitude  $N_1(t, t_1, t_2)$  is given by a sum of four unitarity terms (Fig. 12). Therefore,  $A(s,t)$  takes the form

$$A(s,t) \propto \sum_{i,j} \frac{-i}{s} \int d\Omega_i \left\{ B_i^U \left(\frac{s}{i}\right)^{\phi_1} C_j^U \right\} \left\{ B_i^{L*} \left(\frac{s}{i}\right)^{\phi_2} C_j^{L*} \right\} , \quad (22)$$

a sum of all possible unitarity cuts on the left side of the diagram times all possible cuts on the right.

### C. Diagrams Without Cuts

We now pass on to diagrams that do not have cuts. The essential point we shall demonstrate is that a diagram has a cut if it has third double spectral functions on its sides. As we shall see in Sec. III, this will tie in conveniently with our physical ideas about the composite structure of physical particles.

To demonstrate this relation we will show that the amplitude of any diagram with two-Reggeon exchange (Fig. 13) can be brought to the form

$$A(s,t) \propto \int dK\left(\frac{s}{i}\right)^{\phi_1 + \phi_2 - 1} N_1 N_2, \quad (23a)$$

where  $N_i$  is related<sup>26</sup> to the amplitude of the blobs

$$N_1(t, t_1, t_2) \sim \int_{-\infty}^{+\infty} ds_1 A_1(s_1, t; t_1, t_2). \quad (23b)$$

Furthermore, if  $A_1$  has a third double-spectral function, then the integral in Eq. (23b) is nonzero. But if  $A_1$  has no third double-spectral function, then  $N_1$  is identically zero; in this case, Eq. (23a) is also zero and the leading behavior of  $A(s,t)$  is of lower order in  $s$  than Eq. (23a).

We saw earlier that the leading behavior of the AFS diagram vanishes as  $s \rightarrow \infty$ . (It behaves as  $\ln s/s^3$ .) Its amplitude can be brought to the form of Eq. (23a), even though the coefficients  $N_1, N_2$  are zero. To do this, apply the Gribov analysis to Fig. 3:

$$\begin{aligned}
 d_1 &= (p_1 - k)^2 = (1 - \beta) \left( \frac{m^2}{s} - \alpha \right) s + K^2 - m^2 + i\epsilon \\
 d_2 &= (p_2 + k)^2 = (1 + \alpha) \left( \frac{m^2}{s} + \beta \right) s + K^2 - m^2 + i\epsilon .
 \end{aligned}
 \tag{23c}$$

Then  $d_1, d_2 \sim O(\Lambda)$  gives  $\alpha \sim \beta \sim O(\Lambda/s)$ ; setting  $\alpha \rightarrow \alpha s$ ,  $\beta \rightarrow \beta s$ , we have

$$d_1 = -\alpha + K^2 + i\epsilon, \quad d_2 = \beta + K^2 - i\epsilon, \quad t_1 = K^2, \quad t_2 = (K - Q)^2 .$$

Since we have kept  $d_1, d_2$  finite as  $s$  went to infinity, we can write the Regge amplitudes in factorized form,

$$R = g_1(d_1, t_1) \left( \frac{s}{i} \right)^{\phi_1(t_1)} g_2(d_2, t_2), \quad R' = g'_1(d_1, t_1) \left( \frac{s}{i} \right)^{\phi_2(t_2)} g'_2(d_2, t_2).$$

The amplitude takes the form of Eq. (23a) with

$$N_1(t, t_1, t_2) = \int_{-\infty}^{+\infty} d\alpha \frac{g_1}{d_1} g'_1 = \int_{-\infty}^{+\infty} ds_1 A_1(s_1, t; t_1, t_2). \tag{24}$$

In Eq. (24) the integrand, as a function of  $\alpha$ , has pole and cut singularities in the lower half plane (Fig. 14). Since the form factors decrease as  $d_1 \rightarrow \infty$ ,

$$g_1(d_1, t_1) \rightarrow 0 \quad \text{as} \quad d_1 \rightarrow \infty ,$$

we can close the  $\alpha$  contour of integration in the upper half plane and get for  $N_1$  zero, as expected. We conclude that Eq. (23) holds for the AFS amplitude, but its value is zero.

In the discussion of the AFS diagram, we need to invoke properties of the form factors in order to prove that the amplitude does not persist. For the diagram of Fig. 15a we must also employ knowledge of

the form factors. However, for diagrams more complicated (Fig. 20 for example), the absence of the cut rests completely on the absence of the third double-spectral functions.

Consider Fig. 15a. After performing the finite-mass analysis, we arrive at Eq. (23) with

$$A_1 = \int_0^1 d\beta_1 \int_{-\infty}^{+\infty} \frac{d\alpha_1 dK_1}{d_1 d_2 d_3 d_4} \beta_1^{\phi_1 + \phi_2} g_1(d_1, d_3, t_1) \times g_1'(d_3, d_4, t_2) . \quad (25a)$$

As a function of  $s_1$ ,  $A_1$  has only a right hand cut in the lower half plane, so in Eq. (23b) we are tempted to close the  $s_1$  contour of integration in the upper half plane (Fig. 15b). This cannot be done if we ignore the form factors, because the amplitude without form factors satisfies

$$\bar{A}_1(s_1, t; t_1, t_2) \rightarrow \ln s_1 / s_1 . \quad (25b)$$

Therefore, the contour cannot necessarily be closed. We must invoke the presence of the form factors. We do this by interchanging the orders of integration in Eq. (23b) and first integrating on  $\alpha$  ( $\sim -s_1$ ). Then

$$N_1 = \int \frac{d\beta_1 d\alpha_1 dK_1}{d_1 d_2 d_4} \beta_1^{\phi_1 + \phi_2} \int_{-\infty}^{+\infty} \frac{d\alpha g_1 g_2}{d_3} . \quad (25c)$$

The  $\alpha$  integrand has singularities in  $\alpha$  in the upper half plane. The contour can be closed in the lower half plane. Since  $g_1, g_2$  decrease



as  $d_3$  becomes large, we see that the  $\alpha$  integral is zero. The remaining integrals in Eq. (25c) converge, and hence  $N_1 = 0$ .

Finally, we discuss the diagram of Fig. 16, which will lead to the general case of Sec. D. We obtain Eq. (38), with

$$A_1 = \int \frac{d\alpha_1 d\beta_1 dK_1 d\alpha_2 d\beta_2 dK_2}{\prod_1 d_i} \beta_1^{\phi_1} \beta_2^{\phi_2} g_1 g_1' \quad (26)$$

Again,  $A_1$  has only a right cut, but now the amplitude without form factors satisfies

$$\bar{A}_1 \rightarrow \ln s_1 / s_1^2 \quad \text{as } s_1 \rightarrow \infty,$$

and hence the contour of integration in Eq. (23b) can be closed in the upper half plane to give  $N_1 = 0$ . For Fig. 16 the absence of the cut is thrown entirely on the absence of the third double-spectral function.

## D. The General Case

We now come to a general class of two-Reggeon exchange diagrams which is the basis for our derivation of the absorption model. Just how general can this class be? What we are interested in is the amplitude for a diagram of the type of Fig. 13. However, we do not wish the amplitudes  $A_i$  to be completely arbitrary, because in the form of the absorption model we are interested in we require that they be strictly low-energy amplitudes relative to  $s$ . That is, we require that the incident energy  $s$  flow across the Reggeons and not down the sides of the diagram, because we will want to identify the  $A_i$  with direct-channel physical particles near mass shell.

Note that the diagrams we have studied satisfy this condition. For example, we have found that whereas the 4-momenta on the sides of the diagrams can become large (e.g.,  $k_1 = \beta_1 p_1' + \alpha_1 p_2' + K_1$ ,  $0 < \beta_1 < 1$ ,  $\alpha_1 \sim \frac{\Lambda}{s}$ ) the energies  $s_i$  always remain finite relative to  $s$  (e.g.,  $s_1 = -\alpha s + m^2 + K^2$ ,  $\alpha \sim \Lambda/s$ ). The large energy  $s$  flows only across the Reggeons.

It is not hard to convince oneself that a general type of diagram satisfying these conditions is that of Fig. 17 below. The effect of the elementary lines  $1, 2$  is to tell us where the internal Reggeon line ends and to prevent  $A_1$  from having Regge behavior in  $s$ .

Thus, Fig. 17 excludes all the diagrams of Fig. 18. It includes all the diagrams discussed before. (For the double cross diagram,  $A'_1$  would be various  $\delta$  functions.) It also includes the diagram of Fig. 19, if the lines  $n_i$  are grouped into a single line of mass  $M$ . Most important, it includes the diagram of Fig. 20a. When the rungs in the direct channel are summed over, this provides a model for the Regge box diagram of Fig. 20b (first introduced by Arnold and discussed in HPKR).

We consider, then, the diagram of Fig. 17. We use the notation

$$A = A(s,t), \quad A_1 = A_1(s_1,t; t_1,t_2), \quad A'_1 = A_1(s_1,t'_1,u'_1; d_i).$$

The amplitude  $A'_1$  is to be quite general; we are interested only in whether or not it has a third double spectral function, and so write it in the form

$$A'_1 = \int_{4m^2}^{\infty} d\zeta \frac{f(s_1,\zeta)}{\zeta - t'_1} + \int_{4m^2}^{\infty} d\zeta \frac{g(s_1,\zeta)}{\zeta - u'_1}. \quad (27a)$$

That is, we can treat  $A'_1$  as a propagator of mass  $\zeta \geq 4m^2$ . The analysis now goes through as before. We indicate the essential features.

After the finite mass analysis has been performed,  $A(s,t)$  takes the expected form of Eq. (23a,b) with

$$A_1(s_1,t; t_1,t_2) = \int_0^1 d\beta_1 d\beta_2 \int_{-\infty}^{+\infty} \frac{d\alpha_1 d\alpha_2 dK_1 dK_2}{\prod_{i=1}^5 d_i} \beta_1^{\phi_1} \beta_2^{\phi_2} g_1 g_2 A'_1, \quad (27b)$$

where

$$\begin{aligned}
 d_1 &= \alpha_1 \beta_1 + K_1^2 - m^2 + i\epsilon, \\
 d_2 &= (\alpha_1 - m^2)(\beta_1 - 1) + K_1^2 - m^2 + i\epsilon, \\
 d_3 &= (\alpha_1 - \alpha)\beta_1 + (K_1 - K)^2 - m^2 + i\epsilon, \\
 d_4 &= \alpha_2 \beta_2 + K_2^2 - m^2 + i\epsilon, \\
 d_5 &= (\alpha_2 + t - m^2)(\beta_2 - 1) + (Q + K_2)^2 - m^2 + i\epsilon, \\
 d_6 &= (\alpha_2 + t - \alpha)\beta_2 + (K_2 + Q - K)^2 - m^2 + i\epsilon, \\
 s_1 &= -\alpha + K^2 + m^2, \quad u_1 = m^2 + \alpha - t + (K - Q)^2, \quad (28) \\
 t'_1 &= (\alpha_2 + t - \alpha_1)(\beta_2 - \beta_1) + (K_2 + Q - K_1)^2, \\
 u'_1 &= (\alpha_1 + \alpha_2 + t - \alpha - m^2)(\beta_1 + \beta_2 - 1) + (K_1 + K_2 + Q - K)^2.
 \end{aligned}$$

We consider separately the cases of the  $t'_1$  and  $u'_1$  dispersion contributions.

#### The $u'_1$ Contribution

As before, the first task is to establish the analytic properties of the amplitude  $A_1$ . This can again be done by introducing Feynman parameters.

The amplitude  $A_1$  takes the form

$$A_1(s, u_1; t_1, t_2) = \int_{4m^2}^{\infty} d\xi f(s_1, \xi) F_1(s_1, u_1; t_1, t_2, \xi), \quad (29a)$$

$$F_1 = \int_0^{\infty} d\lambda_1 \dots d\lambda_7 [\beta_1(\lambda)]^{\phi_1} [\beta_2(\lambda)]^{\phi_2} \times \frac{e^{iD(\lambda, s_1, u_1, \xi)/c(\lambda)}}{[c(\lambda)]^2} \quad (29b)$$

$$\propto \int_0^1 d\alpha_1 \dots d\alpha_7 \delta(1 - \sum \alpha_i) \frac{c(\alpha)}{[D(\alpha, s_1, u_1, \xi)]^3} \times [\beta_1(\alpha)]^{\phi_1} [\beta_2(\alpha)]^{\phi_2}, \quad (29c)$$

where

$$\beta_1(\alpha) = \frac{\alpha_2(\alpha_4 + \alpha_5 + \alpha_6 + \alpha_7) + \alpha_7(\alpha_4 + \alpha_6)}{c(\alpha)}, \quad (29d)$$

$$\beta_2(\alpha) = \frac{\alpha_5(\alpha_1 + \alpha_2 + \alpha_3 + \alpha_7) + \alpha_7(\alpha_1 + \alpha_3)}{c(\alpha)}, \quad (29e)$$

$$c(\alpha) = \sum_{i=1}^7 \alpha_i, \quad (29f)$$

$$\begin{aligned}
D = & s_1 [\alpha_2 \alpha_3 (\alpha_4 + \alpha_5 + \alpha_6 + \alpha_7) + \alpha_5 \alpha_6 (\alpha_1 + \alpha_2 + \alpha_3 + \alpha_7) + \alpha_2 \alpha_5 \alpha_7 + \alpha_3 \alpha_6 \alpha_7] \\
& + u_1 \alpha_1 \alpha_4 \alpha_7 \\
& + m^2 [\alpha_1 \alpha_2 (\alpha_4 + \alpha_5 + \alpha_6 + \alpha_7) + \alpha_1 \alpha_6 \alpha_7] \\
& + m^2 [\alpha_4 \alpha_5 (\alpha_1 + \alpha_2 + \alpha_3 + \alpha_7) + \alpha_3 \alpha_4 \alpha_7] \\
& + k^2 [\alpha_1 \alpha_3 (\alpha_4 + \alpha_5 + \alpha_6 + \alpha_7) + \alpha_1 \alpha_5 \alpha_7] \\
& + (q - k)^2 [\alpha_4 \alpha_6 (\alpha_1 + \alpha_2 + \alpha_3 + \alpha_7) + \alpha_3 \alpha_4 \alpha_7] \\
& - [\alpha_7 \xi + \sum_1^6 \alpha_i \cdot m^2] \\
\chi & [(\alpha_1 + \alpha_2 + \alpha_3)(\alpha_4 + \alpha_5 + \alpha_6) + \alpha_7(\alpha_1 + \alpha_2 + \alpha_3 + \alpha_4 + \alpha_5 + \alpha_6)] .
\end{aligned}
\tag{29g}$$

The analytic properties of  $A_1$  now follow easily. First,  $A_1$  has all the singularities that  $\bar{A}_1$  has, because they are determined by the Feynman discriminant  $D$  of Eq. (29g). Second,  $A_1$  does not have any new singularity arising from the  $\beta_i$  factors. If  $\beta_1$  vanishes, say, then various  $\alpha_j$  in Eq. (29d) also vanish. Further, since we have assumed  $\phi_1 > -1$ ,  $\beta_1^{\phi_1}$  is integrable; therefore, we are only interested in those singularities in which the propagators  $d_1, \dots, d_6$  also participate. This means that all the remaining  $\alpha_j$ 's must either vanish or pinch. However, these are just the conditions for a Landau singularity of the Feynman amplitude  $\bar{A}_1$ . We conclude that any singularity of  $A_1$  associated with the vanishing of  $\beta_1$  must already be a singularity of  $\bar{A}_1$ . Since the sheet structure of the

singularities is determined by the  $i\epsilon$  prescription in  $D$ , and is unaffected by the presence of the  $\beta_1^{\phi_1}$ , we see that  $A_1$  has no more singularities than  $\bar{A}_1$ .

Third, it is easily seen from Eq. (29g) that  $D$  is strictly negative for  $s_1, u_1 < 2m^2$ ; hence  $A_1$  is real in this region.

So we conclude that  $A_1$  has the same real analytic properties as  $\bar{A}_1$ .

Now we can return to  $N_1$  and bring it to the unitarity form. Since  $A_1$  has left and right thresholds (Fig. 9), we can close the contour of integration around the right cut to obtain (see Fig. 21)

$$N_1 = \sum_i \int_{\Delta_i}^{\infty} ds_1 \text{disc}[A_1] = 2i \sum_i \int_{\Delta_i}^{\infty} ds_1 B_i^U B_i^{L*}. \quad (30)$$

The sums in Eq. (30) are over all possible  $s_1$  channel unitarity cuts with thresholds  $\Delta_j$ .

The amplitude  $A$  becomes

$$A(s,t) = -2i \sum_{i,j} \int dK ds_1 ds_2 \left\{ B_i^U \left(\frac{s}{i}\right)^{\phi_1} C_i^U \right\} \left\{ B_i^{L*} \left(\frac{s}{i}\right)^{\phi_2} C_i^{L*} \right\}. \quad (31)$$

The  $t_1'$  Contribution

The calculations proceed as before. One again verifies that  $A_1$  has the same real analytic structure as  $\bar{A}_1$ . When we come to consider  $N_1$ , we observe that as a function of  $s_1$  the integrand of Eq. (23b) has singularities that all lie in the lower half plane. (This is another way of saying that  $A_1'$  has no left cut.) Hence we can close the  $s_1$  contour of integration in the upper half plane to get zero. Therefore  $N_1 \equiv 0$ , and  $A(s,t)$  does not persist.



### III. PHYSICAL IMPLICATIONS--COMPOSITENESS, MULTIPLE SCATTERING, AND THE ABSORPTION MODEL

Now consider the relationship between the mathematical results obtained and the physical meaning of compositeness and multiple scattering. It is not hard to see why the AFS diagram does not give the double scattering we would expect. On the one hand, the form of a Reggeon amplitude in Fig. 22 implies a compositeness of the external particles  $M_1$  which is reflected in the form factor dependence on  $M_1$ . It was through just this dependence that the Rothe cancellation occurred. This compositeness is also reflected through the ladder representation of a Reggeon (Fig. 23). On the other hand, when the Reggeon of Fig. 22 is inserted in an AFS diagram, the external particles  $M_1, M_4$  are given elementary particle propagators. We claim it is this inconsistency that deprives the AFS diagram of a cut.

What must be done is either to remove the  $M_1$  dependence from Fig. 22 or to represent the external particles  $M_1$  by more realistic propagators. We would like to discuss the second alternative.

It is our belief, in the spirit of Arnold, HPKR, and Yang, that physical particles are complicated composite objects. In a Bethe-Salpeter framework, for example, one writes the equation of Fig. 24, where the right side represents the physical pole of the left side.

In a scattering process of a physical particle, some of the constituent pieces of matter takes part in the scattering, while the rest stands by as a spectator not taking part. A single scattering process that is drawn as Fig. 25a microscopically looks like Fig. 25b, where the double lines are the physical particles and the single lines

are their constituents. Similarly, a double scattering process that is drawn as Fig. 26b should actually be drawn as Fig. 25b. The incident particle at (1) separates into scattering and spectator constituents. At (2) the constituents unite to form a physical particle in the intermediate state. At (3) the same process occurs again, and the physical particle emerges at (4).

In a field theory model, the intermediate physical particle can be represented by the direct-channel ladders of Fig. 23. We can interpret this as a direct channel Reggeon. This suggests Fig. 27a. From the results of Sec. D, we know Fig. 27a does not have a cut because the sides lack third double spectral functions. Physically, this corresponds to an apparent cancellation between the contributions to  $\int ds_1 A_1(s_1, t; t_1, t_2)$  that come from even- and odd-signature physical particles in an exchange degenerate trajectory. A direct-channel Reggeon with signature is represented as in Fig. 27b. Figure 27a becomes replaced by Fig. 27c, which has a cut.

In a phenomenological calculation, we replace the direct channel amplitudes of Fig. 27c by the known physical particles. Thus, for  $\pi^- p \rightarrow \pi^0 n$ , the contribution  $\int_{4m^2}^{\infty} ds_2 \text{disc } A_2(s_2, t; t_1, t_2)$  is written as in Fig. 28, where we include all recurrences of the  $p$  and continuum states. A typical term contributes

$$\int ds_1 \text{disc} \left\{ \frac{g_{ppn} g_{ppP}}{s_2^2 - m_p^2 + i\epsilon} \right\} \propto i g_{ppn} g_{ppP}$$

The scattering amplitude becomes

$$A(s,t) \propto -\frac{1}{s} \int dK g_{\pi\pi\rho} \left(\frac{s}{i}\right)^{\phi_1} g_{npp} \cdot g_{\pi\pi P} \left(\frac{s}{i}\right)^{\phi_2} g_{ppP} \quad (32a)$$

$$\propto -\frac{1}{s} \int \frac{dt_1 dt_2}{(-\lambda)^{\frac{1}{2}}} M_p(s, t_1) M_{el}(s, t_2) \quad (32b)$$

This is the absorption model.

In HPKR the contributions of the remaining terms of Fig. 28 are assumed to have the same  $s, t$  dependence as Eq. (32b), and are added by multiplying Eq. (32b) by a factor  $\lambda$ . It has been shown<sup>27</sup> that the amplitude for

$$p + p \rightarrow p + \text{anything} \quad (33a)$$

proceeding via Pomeranchuk exchange, may be as large as 50% of the elastic amplitude

$$p + p \rightarrow p + p \quad (33b)$$

This suggests that  $\lambda$  could be about 2.

## IV. COMPARISON WITH THE WORK OF GRIBOV ET AL

In Ref. 28, Gribov and Migdal studied amplitudes generated by the exchange of a Regge pole. Their program is to write a Reggeon field theory that can be solved by summing Reggeon diagrams to determine the scattering amplitude. For example, the amplitude involving the Pomeron and the PP cut is given by Fig. 29. This implies for the absorption model that in addition to the diagrams of Fig. 2 one must consider effects of t-channel iterations in Fig. 30. It is well known that if the diagrams of Fig. 30c are summed, the sum has a pole term related to the pole of Fig. 29a, and a cut term related to the cut of Fig. 29b. Is one double counting by including the pole of Fig. 29a separately? Compelling physical arguments have been given in HPKR for why this is not so, and why the physics of elastic absorption is different from the physics of quantum number exchange.

Gribov and collaborators<sup>28,29</sup> derived the absorption model from diagrams. We compare their derivation with ours. For their discussion of  $N_1$ , they write the equation of Fig. 31. They argue in a general fashion that  $A_1$  has no new singularities or complexity from the presence of the  $\beta_i^{\phi_i}$ . Therefore the discontinuity of  $A_1$  can be calculated as for ordinary amplitudes by cutting the diagram and replacing the lower amplitude by its complex conjugate.

They also give a proof for elastic scattering that  $\lambda > 1$ .

Our approach differs from theirs in that we have attempted to present a specific model for the two-Reggeon diagram that is based on

our physical understanding of compositeness and multiple scattering, and to derive the absorption formula from that model.

Kaidalov and Karnakov<sup>29</sup> have considered the effect of the form factors on the convergence of the  $s_1$  integral for  $N_1$  at infinity.

Ter-Martirosyan<sup>30</sup> has derived the two-Reggeon cut from the AFS diagram by using form factors for the internal Reggeons that are evaluated on mass shell. The Rothe cancellation mechanism is removed, and the contribution from the "elementary" propagators evaluated near mass shell gives the expected form of the cut.

He also considers higher order cuts (Fig. 32), and derives the eikonal formula of Arnold. How do his results affect ours? In a phenomenological absorption model, one needs to consider only the  $\rho P$  cut. All elastic multiple scatterings are grouped into a single  $P$  term, which is parameterized and fit by experiment (Fig. 33a,b). The  $PP_\rho$  cut (Fig. 33c) is found to be small. Any cut involving  $P_\rho$  and a non-Pomeranchon (Fig. 33d) is small because the branch point is well below the  $\rho$  pole.

V. ASSUMPTIONS, CONCLUSIONS, AND  
FUTURE AREAS OF WORK

Assumptions

1. Physical particles are composite objects, and when regarded as Reggeons they have definite signature.
2. Multiple scattering of composite systems can be treated in a Glauber scatterer-spectator approach.
3. The leading behavior of a Feynman amplitude is given by the Gribov finite-mass conditions; the second-order term is down by a factor of  $1/s$  from the leading behavior.

Conclusions

The amplitude for the diagram of Fig. 13, where  $A_i$  are low energy amplitudes relative to  $s$ , is given by the absorption formula

$$\begin{aligned}
 A(s,t) &\propto +i \int dK s^{\phi_1 + \phi_2 - 1} e^{-\frac{i\pi}{2}(\phi_1 + \phi_2)} N_1 N_2 \\
 &\propto -i \int \frac{dK}{s} M_1(s, t_1) M_2(s, t_2) + \dots
 \end{aligned}$$

Future Areas of Work

1. What is the effect of t-channel iterations?
2. What is the relation between the absorption model approach and the bootstrap approach? (See Ref. 31.)
3. Is  $\lambda > 1$ ?

ACKNOWLEDGMENTS

A part of the present work was done with the assistance of Dr. F. Henyey--in particular, the formulation of the finite mass condition, the necessity of proving real analyticity of  $A_1$ , and a discussion of the work by HPKR. We wish to thank Professor Marc Ross for suggesting the present problem and for constant encouragement of its development through many stages over a long period of time. I am also grateful to Dr. G. Kane and Dr. R. Kelly for helpful suggestions.

The work could not have been undertaken without a sustained and fruitful interaction with the Cambridge group. I wish to thank Professor J. C. Polkinghorne, Professor R. J. Eden, Dr. I. T. Drummond, Dr. P. V. Landshoff, Dr. D. I. Olive, Dr. G. Winbow, and Dr. S. Negrine for long and instructive discussions. I am grateful to Professor G. Chew for the hospitality of the Lawrence Radiation Laboratory as an A. E. C. Fellow.

## APPENDIX A. CUTS WITH VENEZIANO AMPLITUDES

An essential condition for the AFS diagram not to have a cut is the presence of the form factors. What happens when the Reggeons are represented as Veneziano amplitudes with no form factors? The amplitude of Fig. 3 becomes

$$A(s,t) = \int \frac{s \, d\alpha \, d\beta \, dK}{d_1 d_2} R(s,t_1) R(s,t_2) \quad , \quad (\text{A.1})$$

where  $d_1$  and  $d_2$  are given by Eq. (23c) and  $t_1 = \alpha\beta s + K^2$ ,  $t_2 = (\alpha + t/s)(\beta - t/s)s + (Q - K)^2$ . There are now no form factors and hence no Gribov finite mass condition, but the integral (A.1) can be evaluated directly.<sup>24,33</sup> We obtain the dominant contribution to (A.1) from the region of integration  $0(m^2/s) \leq \beta < 1$  by evaluating the pole in  $\alpha$  at  $d_1 = 0$ ,

$$\alpha = m^2/s + (m^2 - K^2)/(1 - \beta)s \quad . \quad (\text{A.2})$$

The  $\beta$  integrations can be done to give

$$A(s,t) \propto \int dK s^{\phi(K^2) + \phi((Q-K)^2) - 1} [\ln s + i 0(i)] \quad . \quad (\text{A.3})$$

The first term in the brackets comes from  $0(m^2/s) < \beta < \epsilon$  and corresponds to  $d_2$  going off mass shell ( $\epsilon$  is a small finite number). The second term comes from  $\beta \sim 0(m^2/s)$  when  $d_2$  is on mass shell, and corresponds to the usual AFS cut term. The asymptotic behavior of (A.3) is then

$$A(s,t) \rightarrow s^{j_c(t)} [1 + i0(1/\ln s)] \quad (\text{A.4})$$



where

$$j_c(t) = 2\phi(t/4) - 1 \quad . \quad (A.5)$$

APPENDIX B. AN ALTERNATIVE PROOF OF REAL ANALYTICITY FOR  $A_1$ 

One can also investigate real analyticity of the  $A_1$  amplitudes directly using Sudakov variables. Consider Eq. (11). We see that if  $0 < \beta_1 < 1$ , we can evaluate the  $\alpha_1$  integration directly by closing the  $A_1$  contour in the lower half plane and picking up the residues from  $d_1, d_3$ . Writing  $d_i(j)$  as the value of  $d_i$  at the pole of  $d_j$ , and writing  $D_i(j) = \beta_1 d_i(j)$ , we obtain

$$A_1(s_1, t; t_1, t_2) \propto \iint dK \int_0^1 d\beta_1 \frac{\beta_1^{\phi_1+1} (1-\beta_1)^{\phi_2}}{d_3(1)} \left\{ \frac{1}{D_2(1)D_4(1)} - \frac{1}{D_2(3)D_4(3)} \right\}, \quad (\text{B.1})$$

where

$$\begin{aligned} d_3(1) &= -\alpha\beta_1 + (K_1 - K)^2 - K_1^2 \\ D_2(1) &= -[m^2 - \beta_1(1-\beta_1)(m^2 + \alpha - t)] + (1-\beta_1)K_1^2 + \beta_1(K_1 + Q - K)^2 \\ D_2(3) &= -[m^2 - \beta_1(1-\beta_1)(m^2 - \alpha)] + \beta_1K_1^2 + (1-\beta_1)(K_1 - K)^2 \\ D_4(1) &= -[m^2 - \beta_1(1-\beta_1)(m^2 + \alpha - t)] + (1-\beta_1)K_1^2 + \beta_1(K_1 + Q - K)^2 \\ D_4(3) &= -[m^2 - \beta_1(1-\beta_1)(m^2 - t)] + \beta_1(K_1 - K + Q)^2 + (1-\beta_1)(K_1 - K)^2. \end{aligned} \quad (\text{B.2})$$

We immediately see that at the endpoints of integration--  $\beta_1 = 0, 1$  -- the terms  $D_i(j)$  are strictly negative and cannot vanish. The term

$d_3(1)$  can vanish, but its residue is zero [i.e.,  $d_3(1)$  is a factor of the terms in the brackets]. Hence we conclude that the terms  $\beta_1^{\phi_1}$ ,  $(1 - \beta_1)^{\phi_2}$  do not introduce any new singularities.

Finally, we observe that  $A_1$  is certainly a real quantity when the  $D_i(j)$ 's are negative for all  $\beta_1$  between 0 and 1. This occurs when the terms in brackets of Eq. (B.2) are positive. Since the maximum value of  $\beta_1(1 - \beta_1)$  is  $1/4$ , this condition is satisfied for

$$4m^2 > m^2 + \alpha - t, \quad m^2 - \alpha, \quad m^2 - t.$$

This is equivalent to the region

$$s_1 < 4m^2 + K^2, \quad -3m^2 < t < 0, \quad s_1 + t > -2m^2 + K^2,$$

which overlaps with the region  $D_2$  of Fig. 8.

This method can also be applied to the amplitude  $A_1$  of Fig. 17, but it becomes very tedious. The Feynman parameter method is considerably easier.

FOOTNOTES AND REFERENCES

- \* Preliminary versions of the present work have appeared in Proceedings of the 1969 Regge Cut Conference at Wisconsin, April 23-25, 1969, pp. 30-40, 96-109 (unpublished), and Lawrence Radiation Laboratory Report UCRL-19453, January 14, 1970.

The Sudakov variable techniques, used extensively here, were first applied to diagrams with Reggeons in a comprehensive work to develop a Reggeon calculus by V. N. Gribov (1967). In the work at hand we have employed these techniques to analyze the diagrams considered here in obtaining the absorption model. After our work was completed (August, 1969), a series of six papers by Gribov and Migdal, Kaidalov and Karnakov, and ter-Martirosyan extended the earlier work of Gribov, and, among other things, obtained the absorption model. In Sec. IV we compare our approach with theirs and discuss the similarities and differences.

1. T. Regge, *Nuovo Cimento* 14, 951 (1959).
2. G. E. Hite, *Rev. Mod. Phys.* 41, 669 (1969).
3. R. J. Eden, P. V. Landshoff, D. I. Olive, and J. C. Polkinghorne, The Analytic S-Matrix (Cambridge University Press, 1966).
4. R. J. Eden, High Energy Collisions of Elementary Particles (Cambridge University Press, 1967).
5. F. Henyey, G. L. Kane, J. Pumplin, and M. Ross, *Phys. Rev.* 182, 1579 (1969), hereafter referred to as HKPR.
6. E. S. Abers, H. Burkhardt, V. L. Teplitz, and C. Wilkin, *Nuovo Cimento* 42, 365 (1965).
7. B. M. Udgaonkar and M. Gell-Mann, *Phys. Rev. Letters* 8, 346 (1962).

8. R. J. Glauber, in Lectures in Theoretical Physics (Wiley-Interscience, Inc., New York, 1959), Vol. 1; V. Franco and R. J. Glauber, Phys. Rev. 142, 1195 (1966).
9. A solution to this difficulty, different from the one we present, has been suggested by Dr. C. Wilkin, Graphs and Glauber, University College Preprints.
10. R. C. Arnold, Phys. Rev. 153, 1523 (1967); Argonne National Laboratory Report No. ANL/HEP 6804, 1968 (unpublished).
11. C. B. Chiu and J. Finkelstein, Nuovo Cimento 57A, 649 (1968).
12. D. Amati, S. Fubini, and A. Stanghellini, Phys. Letters 1, 29 (1962).
13. P. G. Federbush and M. T. Grisaru, Ann. Phys. 22, 263, 299 (1963).
14. J. C. Polkinghorne, Phys. Letters 4, 24 (1963).
15. S. Mandelstam, Nuovo Cimento 30, 1127 (1963); 30, 1148 (1963).
16. H. J. Rothe, Phys. Rev. 159, 1471 (1967).
17. C. Wilkin, Nuovo Cimento 31, 377 (1964).
18. This is also easily seen from a d-line analysis of the Reggeon in the ladder representation.
19. V. N. Gribov, in Proceedings of 1967 International Conference on Particles and Fields (Wiley-Interscience Inc., New York 1967); Zh. Eksp. i Teor. Fiz. 53, 654 (1967); [English transl.: Soviet Phys.-JETP 26, 414 (1968)]; V. V. Sudakov, Zh. Eksp. i Teor. Fiz. 30, 87 (1956) [English transl.: Soviet Phys.-JETP 3, 65 (1956)].
20. I. T. Drummond, P. V. Landshoff, and W. J. Zakrzewski, Nucl. Phys. B11, 383 (1969).

21. P. V. Landshoff and J. C. Polkinghorne, Cambridge Preprint 68/29.
22. We are very indebted to P. V. Landshoff for suggesting this approach.
23. J. C. Polkinghorne, Cambridge Preprint 69/31. See also Ref. 24, 25.
24. S. N. Negrine, Cambridge Preprint 69/34.
25. G. A. Winbow, Cambridge Preprint 68/26.
26. J. C. Polkinghorne, Nucl. Phys B6, 441 (1968).
27. J. Pumplin and M. Ross, Phys. Rev. Letters 21, 1778 (1968).
28. V. N. Gribov and A. A. Migdal, Yad. Fiz. 8, 1002, 1213 (1968),  
[English translation: Soviet J. Nucl. Phys. 8, 583,  
703 (1969)].
29. A. B. Kaidalov and B. M. Karnakov, Phys. Letters 29B, 372 (1969).
30. K. A. ter-Martirosyan, I. T. E. P. preprints, summer 1969.
31. L. Caneschi, Phys. Rev. Letters 23, 254 (1969).
32. Veneziano amplitudes in vertex diagrams have been evaluated by  
I. S. Gerstein, Kurt Gottfried, and Kerson Huang, Phys. Rev.  
Letters 24, 294 (1970).
33. The same technique is used for the vertex diagram. Clifford Risk,  
Phys. Rev. July 15, 1970 (to be published).

## FIGURE CAPTIONS

- Fig. 1. Diagrams for  $\pi D$  scattering.
- Fig. 2. Diagrams for absorption model.
- Fig. 3. AFS diagram.
- Fig. 4. Mandelstam diagram.
- Fig. 5. Integration contour for Fig. 3 in the complex  $s_1$  plane.
- Fig. 6. Singularities of the  $\alpha$  integrand in the complex  $\alpha$  plane.  
The integration on  $\alpha$  runs from  $-\infty$  to  $+\infty$ .
- Fig. 7. Diagram for the amplitude  $\bar{A}_1$ . When  $g_1$  and  $\beta_1$  are included, we obtain  $A_1$ .
- Fig. 8. Analytic properties of  $A_1$ ;  $A_1$  has singularities at  $s_1 = 4m^2$ ,  $u_1 = 4m^2$ , and  $f_1 = 0$  (boundary of double spectral function), and it is real in  $D_1$ .
- Fig. 9. (a) Contour of integration for  $N_1$ .  
(b) Representation for  $N_1$  of Fig. 4 in terms of the integral of the absorptive part of  $A_1$ .
- Fig. 10. The single scattering amplitudes  $M_1$ ,  $M_2$  of Eq. (20c).
- Fig. 11. Extension of the Mandelstam diagram.
- Fig. 12. Representation for  $N_1$  of Fig. 11 in terms of the integral of the absorptive parts of  $A_1$ .
- Fig. 13. The general two Reggeon exchange diagram.
- Fig. 14. Contour of integration in  $\alpha$  for  $N_1$  of Fig. 3.
- Fig. 15a. Diagram without a cut.
- Fig. 15b. Contour of integration in  $s_1$  for  $N_1$  of Fig. 15a.
- Fig. 16. Diagram without a cut.

- Fig. 17. The general two Reggeon exchange diagram with low energy direct-channel amplitudes.
- Fig. 18. Diagrams not contained in Fig. 17.
- Fig. 19. A class of diagrams contained in Fig. 17.
- Fig. 20. Representation of the Regge box diagram in terms of diagrams of the class of Fig. 17.
- Fig. 21. Representation of  $N_1$  of Fig. 17 in terms of absorptive parts of  $A_1$ .
- Fig. 22. Regge amplitude with form factors representing composite external particles.
- Fig. 23. Ladder representation of a Reggeon.
- Fig. 24. Bethe-Salpeter representation of composite physical particles.
- Fig. 25. Single scattering of composite systems.
- Fig. 26. Double scattering of composite systems.
- Fig. 27. (a) Two-Reggeon exchange with direct-channel ladders.  
(b) Ladder representation of a direct-channel Reggeon with signature.  
(c) Diagram for two-Reggeon exchange with direct-channel Reggeons with signature.
- Fig. 28. Contributions to the amplitude  $N_2$  from the direct-channel physical states that are contained in  $A_1$ .
- Fig. 29. Graphs in the Reggeon perturbation theory of Gribov and Migdal.



- Fig. 30. Graphs that have not been included in the derivation of the absorption model. These graphs have amplitudes  $A_i$  that have large subenergies.
- Fig. 31. The equation Gribov and Migdal use to relate  $N_1$  to direct channel physical states.
- Fig. 32. S-channel iterations of the Pomeron that give the eikonal.
- Fig. 33. Cuts generated by the  $\rho$ . Diagrams (a), (b) are used in the absorption model; (c), (d) have small contributions.

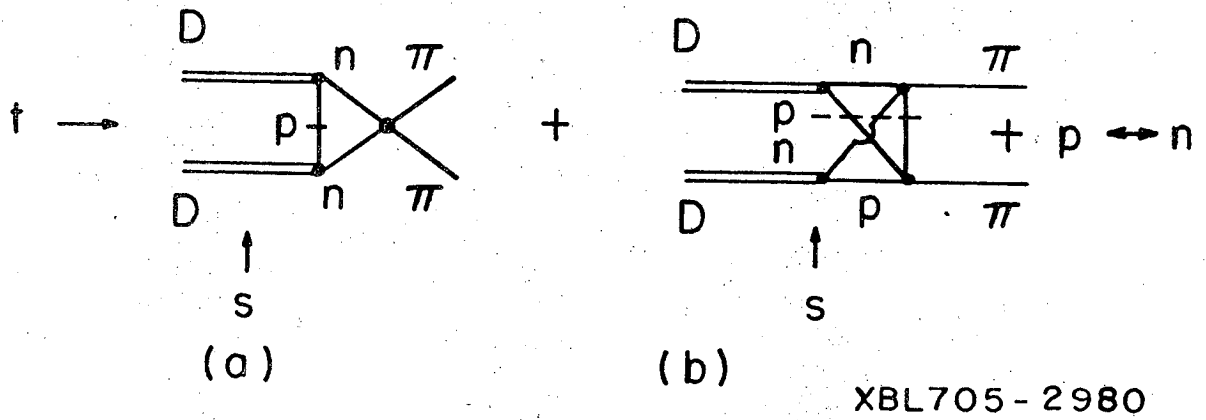
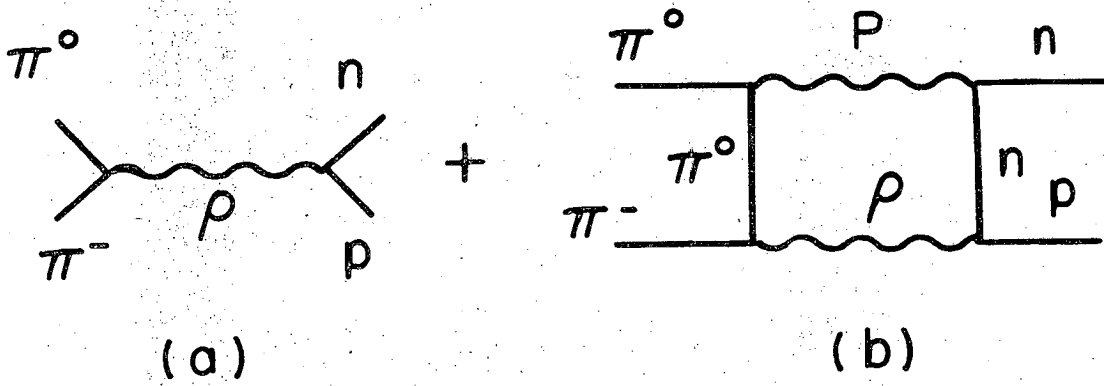
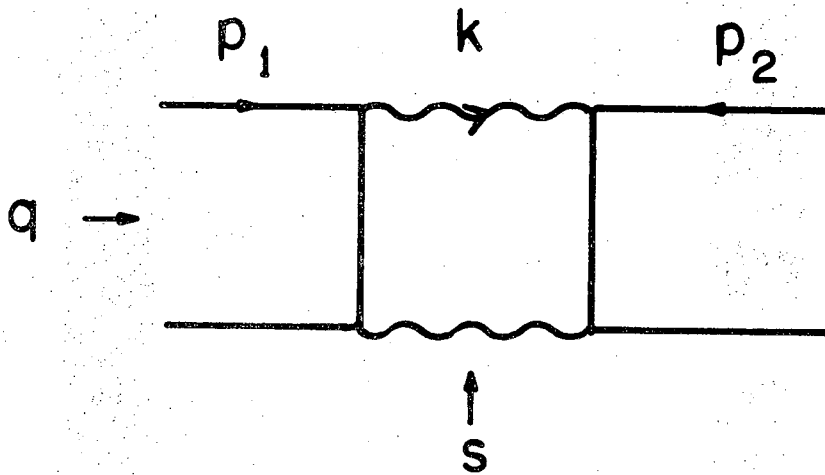


Fig. 1.



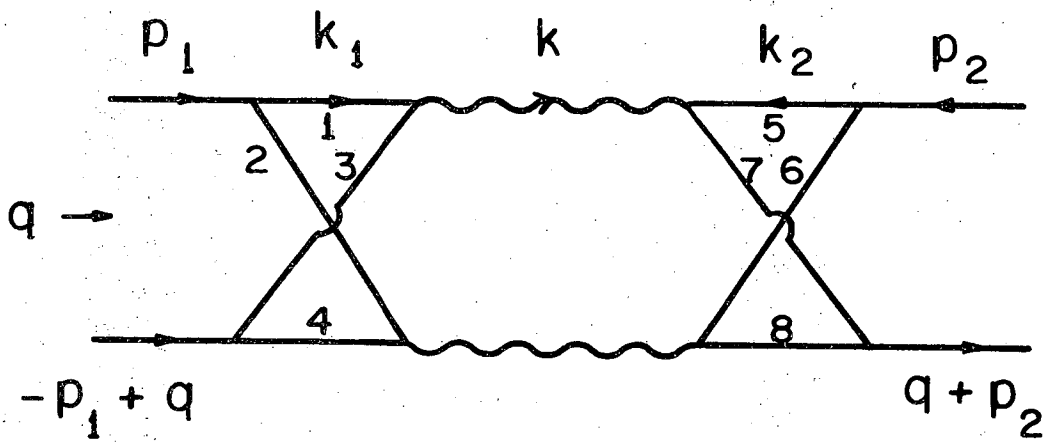
XBL 705 - 2981

Fig. 2.



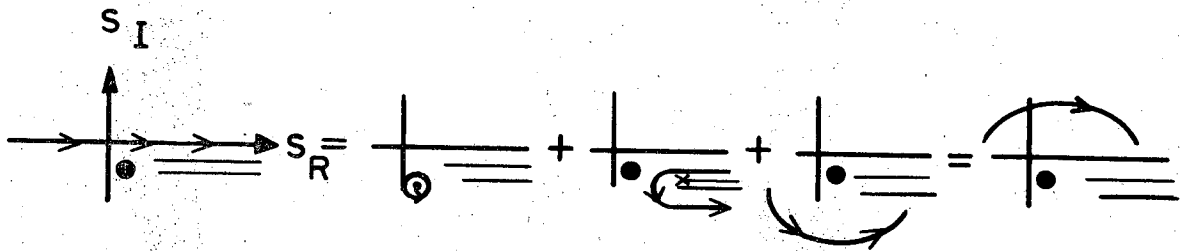
XBL 705 - 2982

Fig. 3.



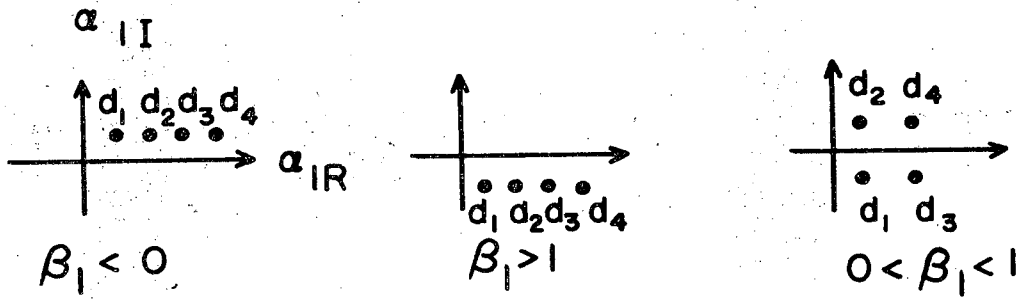
XBL705 - 2983

Fig. 4.



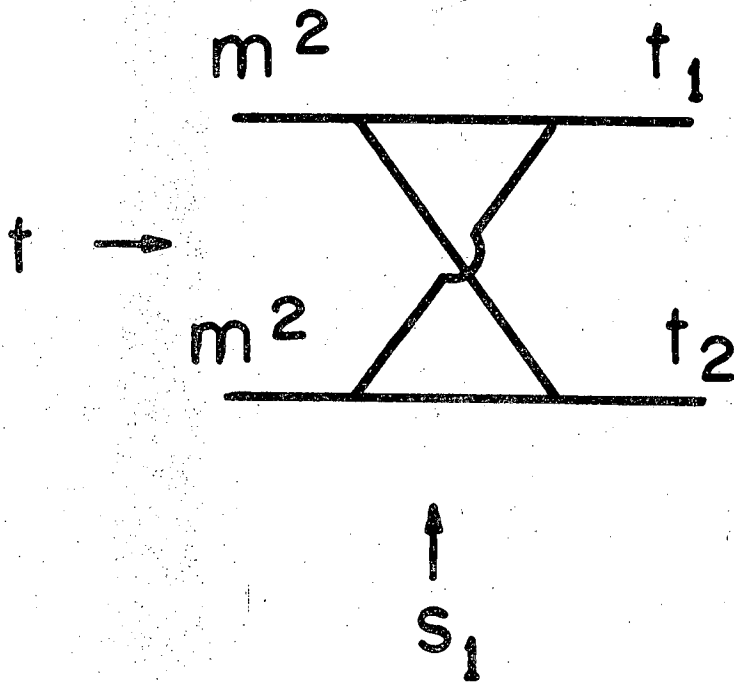
XBL706 - 3093

Fig. 5.



XBL706-3097

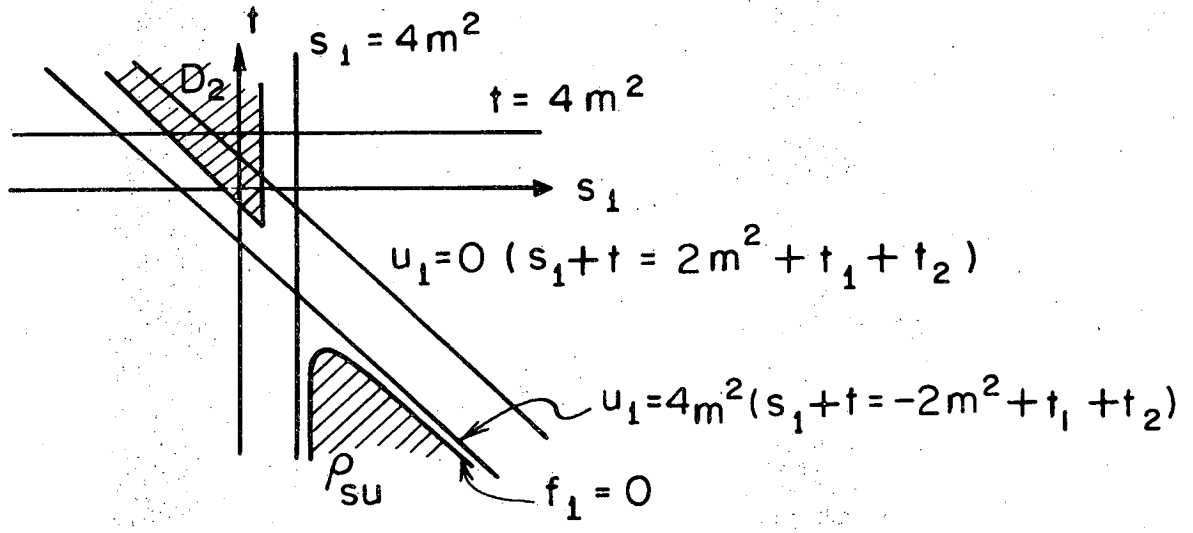
Fig. 6.



XBL705 - 2984

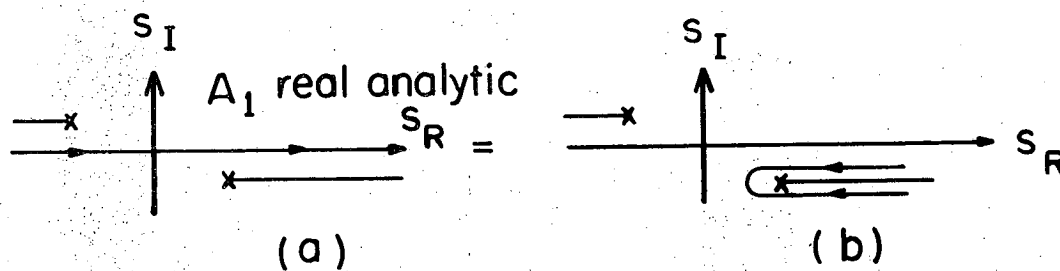
Fig. 7.





XBL705-2985

Fig. 8.



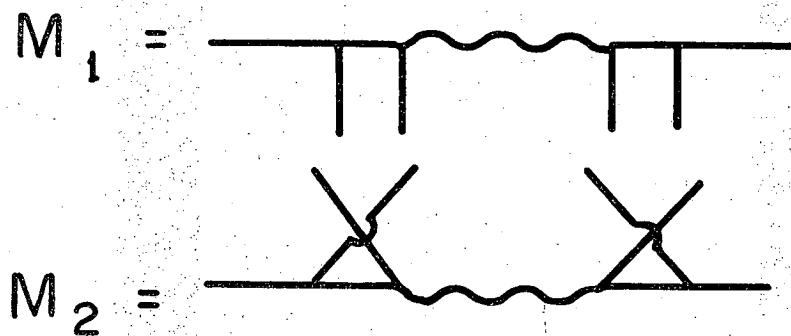
XBL705-2986

Fig. 9a.

$$N_1 = \int_{-\infty}^{+\infty} ds_1 \sum_{\mathbf{k}_1} = \int_{4m^2}^{\infty} ds_1 \sum_{\mathbf{k}_1} = i \int_{4m^2}^{\infty} ds_1 \int d\mathbf{k}_1 \Pi_1^* \sum_{\mathbf{k}_1}^*$$

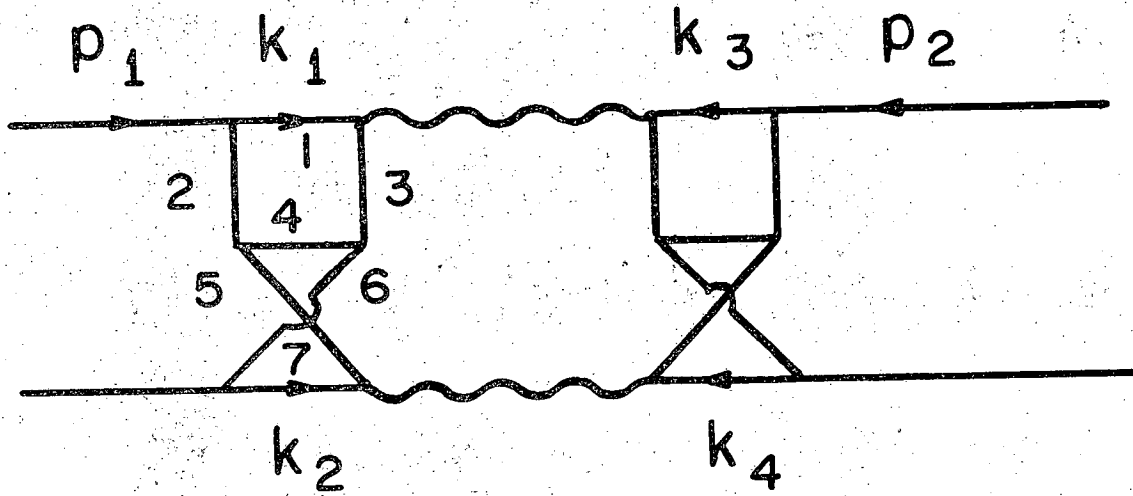
XBL 706-3091

Fig. 9b.



XBL705 - 2988

Fig. 10.



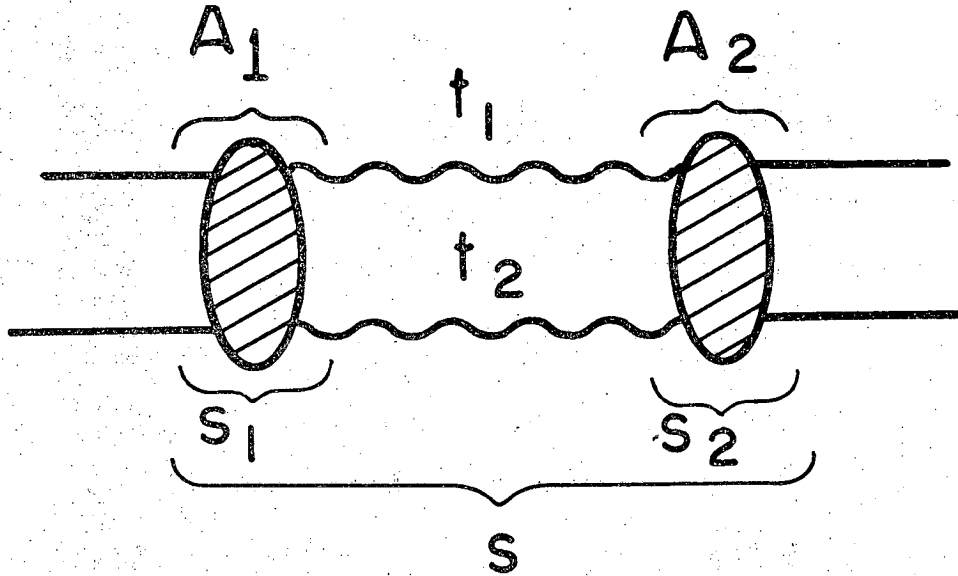
XBL 705-2987

Fig. 11.

$$N_1 = \int_{-\infty}^{+\infty} ds_1 \left\{ \int_{-\infty}^{+\infty} ds_2 \left[ \frac{1}{4m^2} \left( \frac{\partial}{\partial s_1} \frac{\partial}{\partial s_2} \right) \right] + \int_{-\infty}^{+\infty} ds_3 \left[ \frac{1}{9m^2} \left( \frac{\partial}{\partial s_1} \frac{\partial}{\partial s_3} \right) \right] \right\}$$

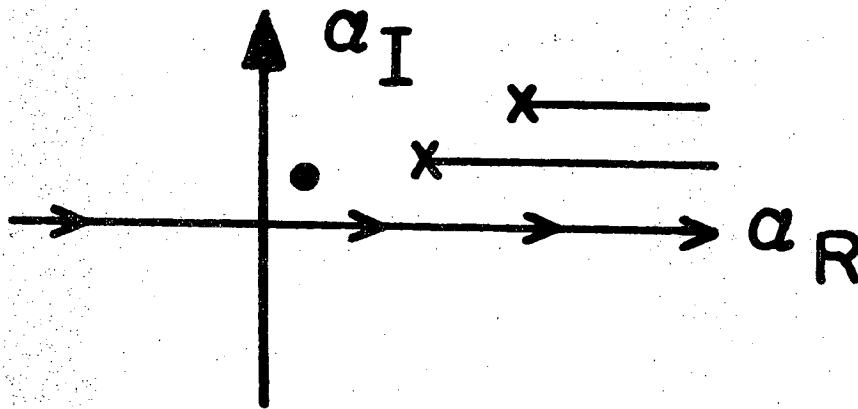
XBL 706 - 3092

Fig. 12.



XBL705-2989

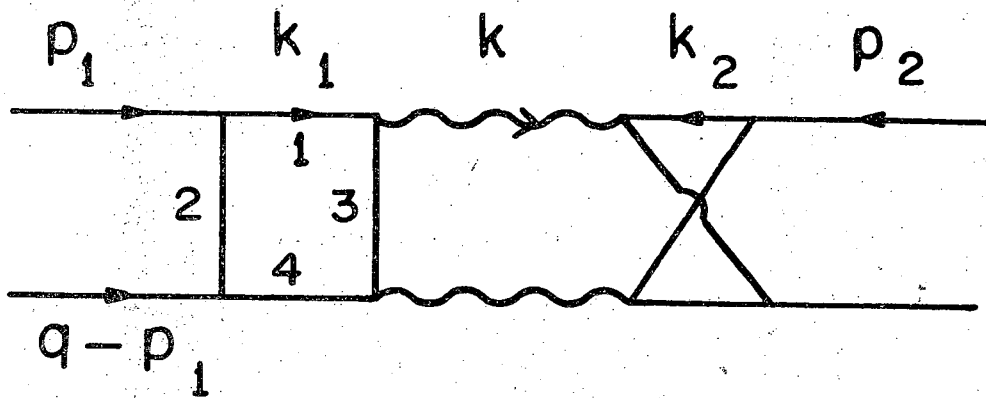
Fig. 13.



XBL706-3099

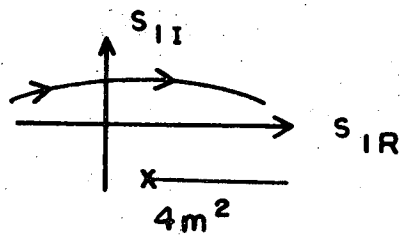
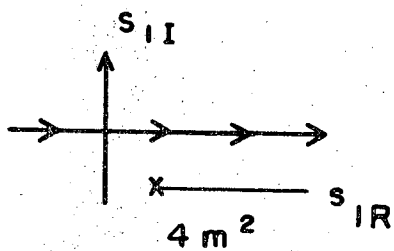
Fig. 14.





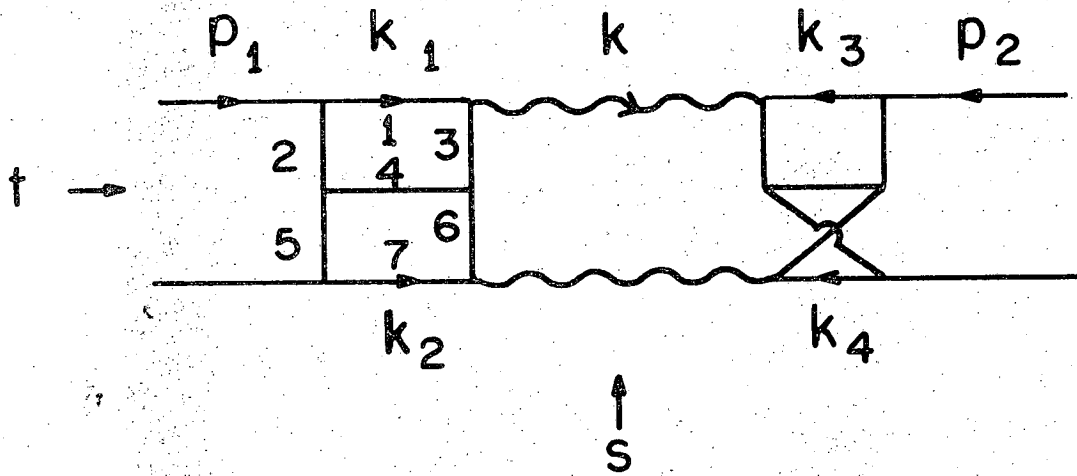
XBL705-2990

Fig. 15a.



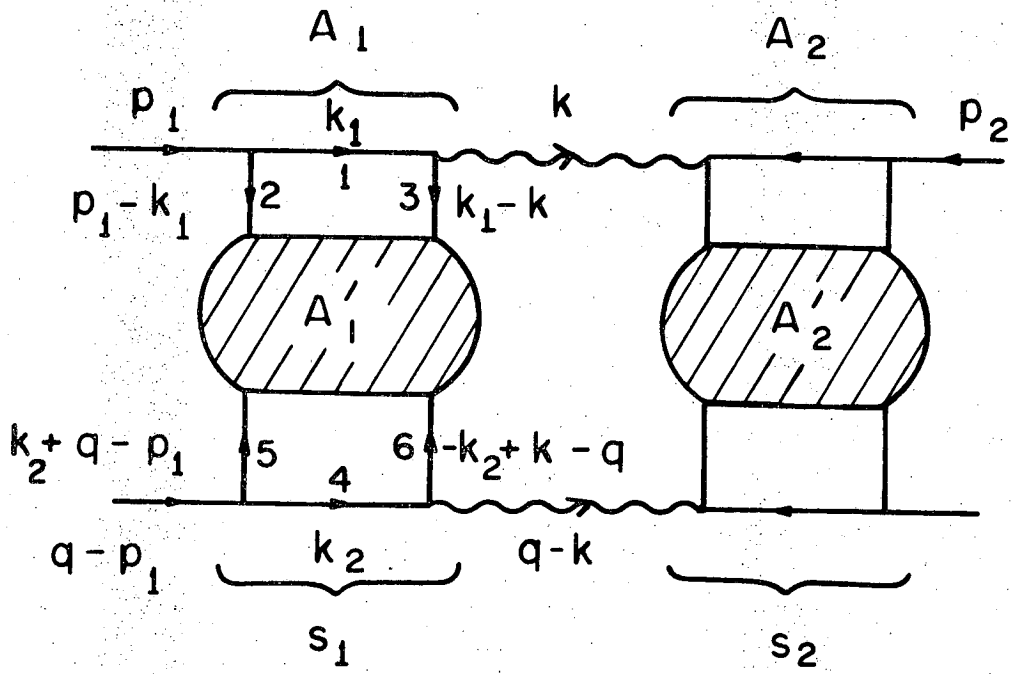
XBL706-3096

Fig. 15b.



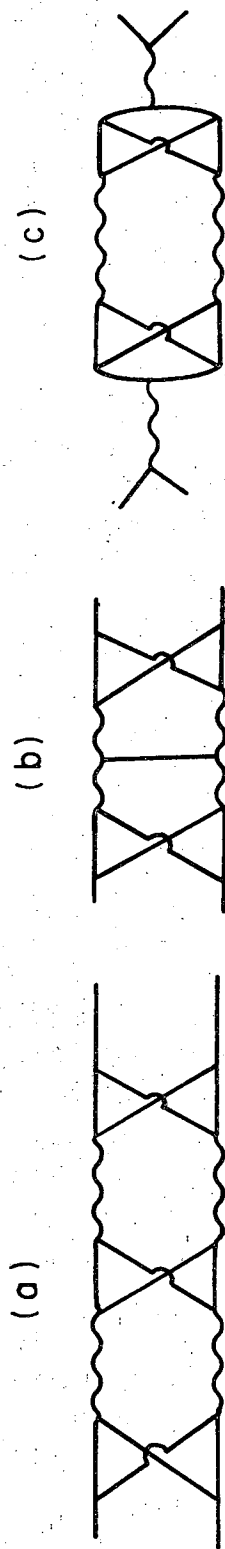
XBL705-2991

Fig. 16.



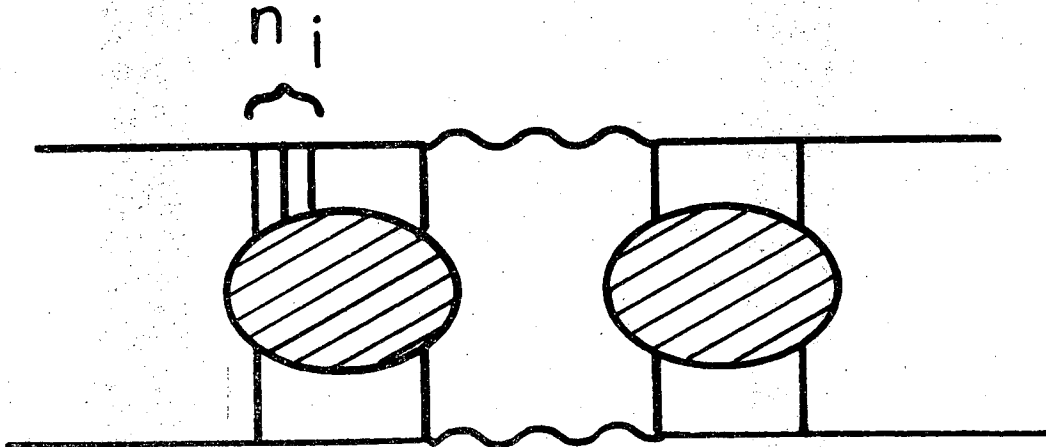
XBL705-2995

Fig. 17.



XBL 705 - 2992

Fig. 18.



XBL 705-2993

Fig. 19.

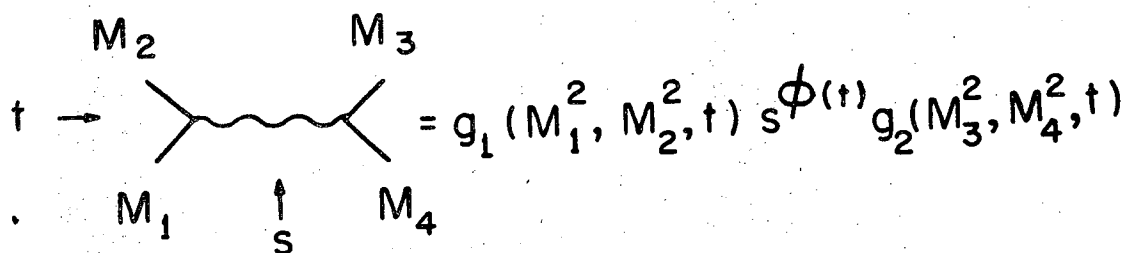


$$N_1 = \int_{4m^2}^{\infty} ds_1 \left\{ \begin{array}{l} \text{Diagram 1} \\ \text{Diagram 2} \\ \text{Diagram 3} \end{array} \right\} + \sum_j \int_{\Delta_j}^{\infty} ds_1 \left\{ \begin{array}{l} \text{Diagram 4} \\ \text{Diagram 5} \\ \text{Diagram 6} \end{array} \right\}$$

XBL706 - 3090

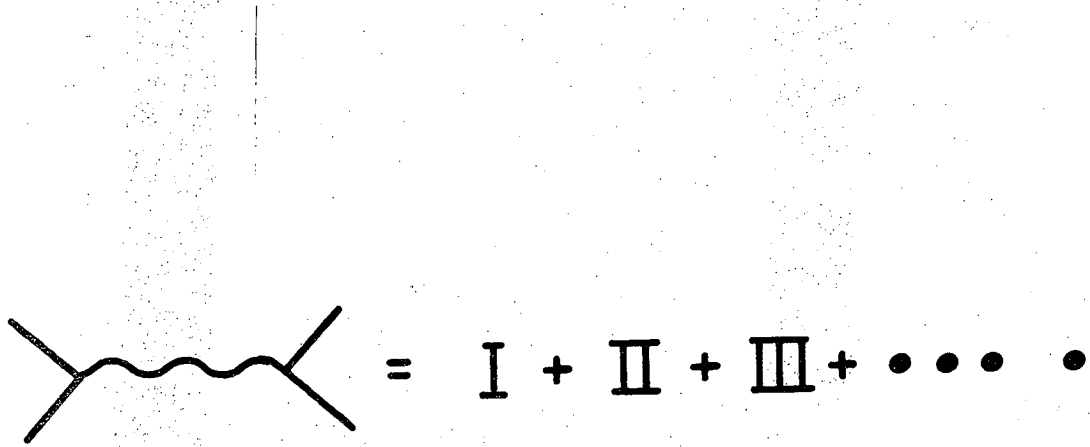
Fig. 21.




$$t \rightarrow \begin{array}{c} M_2 \qquad M_3 \\ \diagdown \quad \diagup \\ \text{---} \text{---} \text{---} \text{---} \text{---} \text{---} \\ \diagup \quad \diagdown \\ M_1 \qquad M_4 \\ \uparrow \\ s \end{array} = g_1(M_1^2, M_2^2, t) s^{\phi(t)} g_2(M_3^2, M_4^2, t)$$

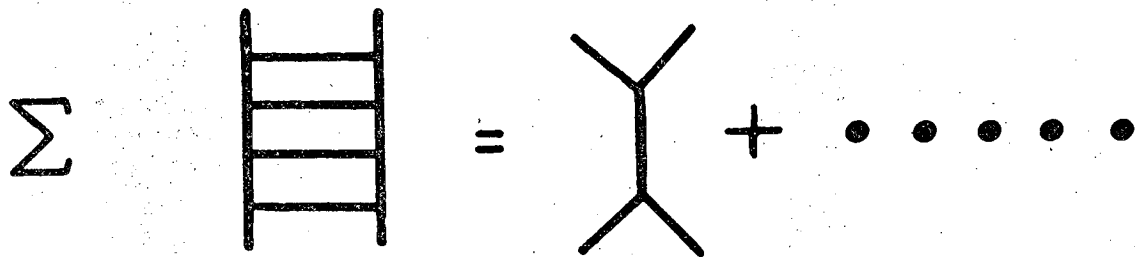
XBL706-3088

Fig. 22.



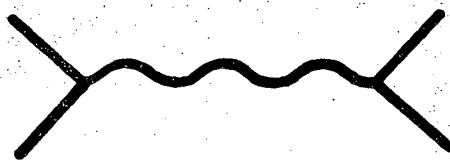
XBL706 - 3089

Fig. 23.

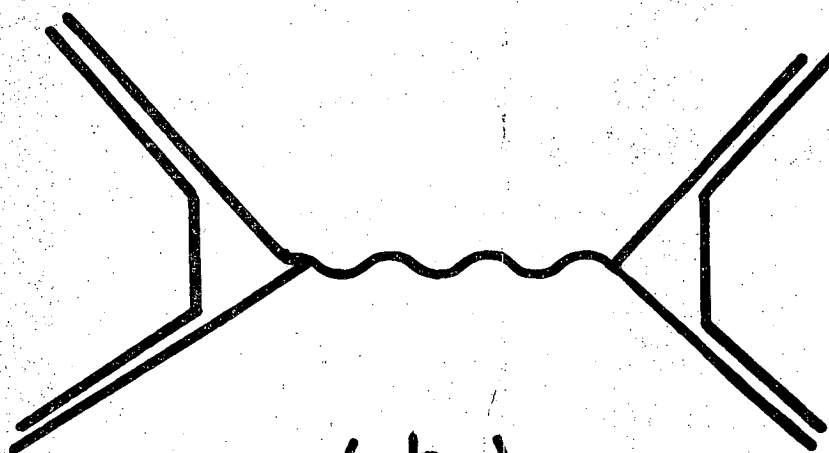


XBL705-2996

Fig. 24.



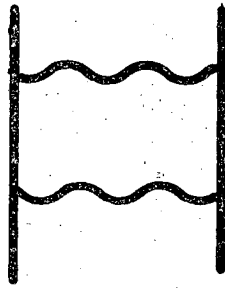
(a)



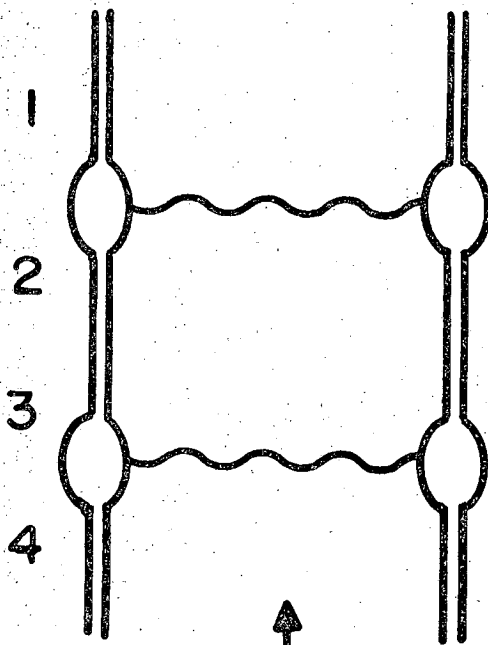
(b)

XBL705-2997

Fig. 25.



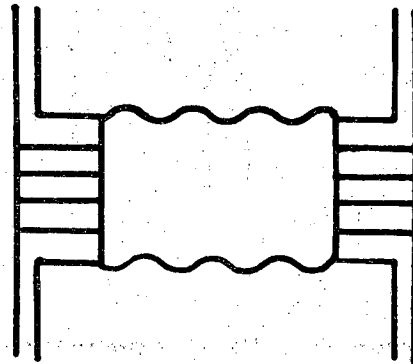
(a)



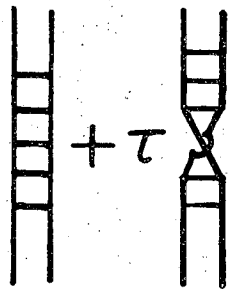
(b) s

XBL705 - 3003

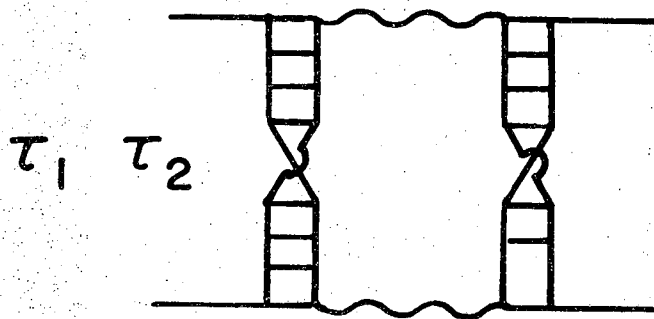
Fig. 26.



(a)



(b)



(c)

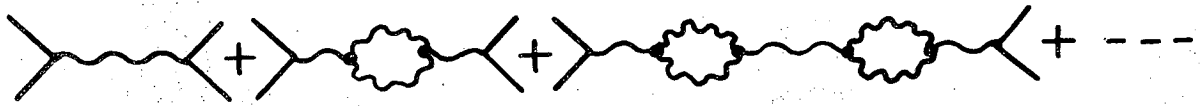
XBL 706 - 2998

Fig. 27.

$$\left. \begin{array}{c} \text{disc} \\ \tau_2 \end{array} \right\} \left. \begin{array}{c} \text{disc} \\ \tau_2 \end{array} \right\} = \text{disc} \left\{ \begin{array}{l} I + I + \dots + p \overline{O} \pi + \dots \\ p N^*_{(1400)} \end{array} \right\}$$

XBL706-3094

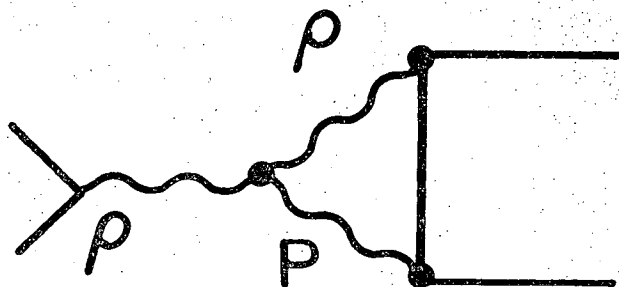
Fig. 28.



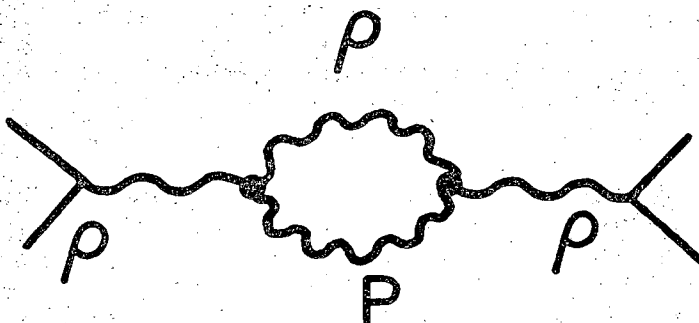
XBL705 - 2999

Fig. 29.

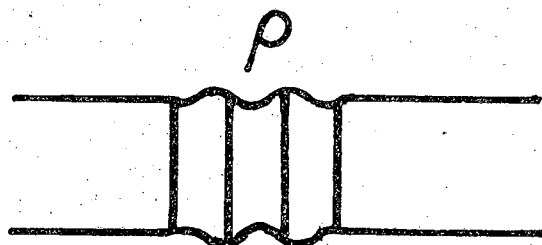




(a)



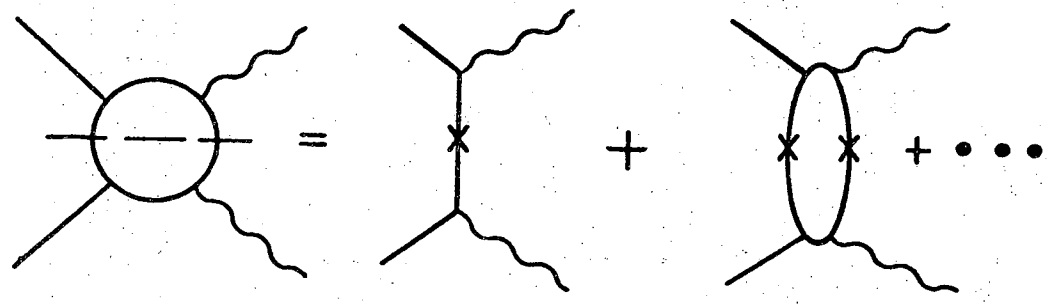
(b)



(c)

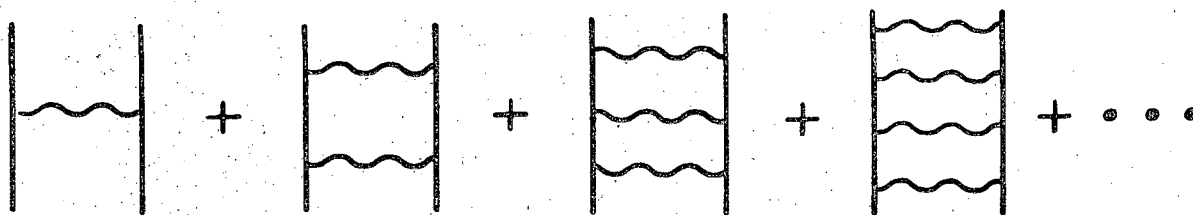
XBL705 - 3000

Fig. 30.



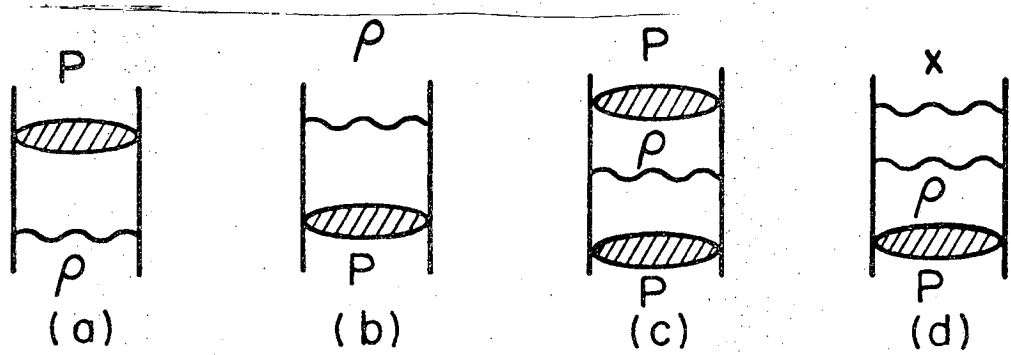
XBL706-3098

Fig. 31.



XBL 705-3001

Fig. 32.



XBL705 - 3002

Fig. 33.

LEGAL NOTICE

*This report was prepared as an account of Government sponsored work. Neither the United States, nor the Commission, nor any person acting on behalf of the Commission:*

- A. Makes any warranty or representation, expressed or implied, with respect to the accuracy, completeness, or usefulness of the information contained in this report, or that the use of any information, apparatus, method, or process disclosed in this report may not infringe privately owned rights; or*
- B. Assumes any liabilities with respect to the use of, or for damages resulting from the use of any information, apparatus, method, or process disclosed in this report.*

*As used in the above, "person acting on behalf of the Commission" includes any employee or contractor of the Commission, or employee of such contractor, to the extent that such employee or contractor of the Commission, or employee of such contractor prepares, disseminates, or provides access to, any information pursuant to his employment or contract with the Commission, or his employment with such contractor.*

TECHNICAL INFORMATION DIVISION  
LAWRENCE RADIATION LABORATORY  
UNIVERSITY OF CALIFORNIA  
BERKELEY, CALIFORNIA 94720